USGS
science for a changing world

Prepared in cooperation with
FALLON PAIUTE-SHOSHONE TRIBE

Characterization of Surface-Water Quality in the S-Line Canal and Potential Geochemical Reactions from Storage of Surface Water in the Basalt Aquifer near Fallon, Nevada

Scientific Investigations Report 2005–5102

U.S. Department of the Interior
U.S. Geological Survey

COVER: View looking north of the top of Rattlesnake Hill. Photograph taken by Douglas K. Maurer, 2001.

Characterization of Surface-Water Quality in the S-Line Canal and Potential Geochemical Reactions from Storage of Surface Water in the Basalt Aquifer near Fallon, Nevada

By Alan H. Welch, Douglas K. Maurer, Michael S. Lico, and John K. McCormack

Prepared in cooperation with the
FALLON PAIUTE-SHOSHONE TRIBE

Scientific Investigations Report 2005–5102

U.S. Department of the Interior
U.S. Geological Survey

U.S. Department of the Interior
Gale A. Norton, Secretary

U.S. Geological Survey
P. Patrick Leahy, Acting Director

U.S. Geological Survey, Carson City, Nevada: 2005

For sale by U.S. Geological Survey, Information Services
Box 25286, Denver Federal Center
Denver, CO 80225

For more information about the USGS and its products:
Telephone: 1-888-ASK-USGS
World Wide Web: http://www.usgs.gov/

For additional information contact:

Director
USGS, Nevada Water Science Center
333 W. Nye Lane, Room 203
Carson City, NV 89706-0866

email: GS-W-NVpublic-info@usgs.gov

http://nevada. usgs.gov

Contents

Figures

Tables

Conversion Factors and Datums

Multiply	By	To obtain
	Length	
inch (in.)	2.54	centimeter (cm)
foot (ft)	0.3048	meter (m)
mile (mi)	1.609	kilometer (km)
liter	33.82	ounce
square foot per pound (ft^2/lb)	0.00278	square meters per gram (cm^2/g)
	Flow rate	
acre-foot per year (acre-ft/yr)	1,233	cubic meter per year (m^3/yr)
foot per year (ft/yr)	0.3048	meter per year (m/yr)
cubic foot per second (ft^3/s)	0.02832	cubic meter per second (m^3/s)

Water quality and other units used in this report:

g/µg	gram per microgram	mg/kg	milligram per kilogram
g/cm^3	gram per cubic centimeter	mg/L	milligram per liter
g/mol	gram per mol	mol/mol	mole per mole
g/L	gram per liter	mol/L	mole per liter
µm	micrometer	mm	millimeter
µg/L	microgram per liter	nm	nanometer
µS/cm	microsiemens per centimeter at 25°C	pCi/L	picocuries per liter
mg/g	milligram per gram		

Temperature in degrees Celsius (°C) may be converted to degrees Fahrenheit (°F) as follows:

$°F=(1.8\times°C)+32$

Temperature in degrees Fahrenheit (°F) may be converted to degrees Celsius (°C) as follows:

$°C=(°F-32)/1.8$

In this report, "sea level" refers to the National Geodetic Vertical Datum of 1929 (NGVD of 1929, formerly called "Sea-Level Datum of 1929"), which is derived from a general adjustment of the first-order leveling networks of the United States and Canada.

Characterization of Surface-Water Quality in the S-Line Canal and Potential Geochemical Reactions from Storage of Surface Water in the Basalt Aquifer near Fallon, Nevada

By Alan H. Welch, Douglas K. Maurer, Michael S. Lico, and John K. McCormack

Abstract

The Fallon basalt aquifer serves as the sole source of municipal water supply for the Lahontan Valley in west-central Nevada. Principal users include the City of Fallon, Naval Air Station Fallon, and the Fallon Paiute-Shoshone Tribe. Pumpage from the aquifer increased from about 1,700 acre-feet per year in the early 1970's to more than 3,000 acre-feet per year in the late 1990's, and has been accompanied by declines in water levels and changes in water quality. Storage of surface water in the basalt may mitigate the effects of pumpage, but may cause undesirable changes in water chemistry. In May 2001, the U.S. Geological Survey began a study, in cooperation with the Fallon Paiute-Shoshone Tribe, to characterize the surface-water quality of the S-Line Canal, a likely source of water for augmenting recharge. Because arsenic concentrations in ground water of the basalt aquifer exceed drinking water standards, the potential for arsenic release to artificial recharge was explored by using geochemical modeling. Model results suggest that arsenic release may increase concentrations to levels that could limit the use of artificial recharge. Field-based experiments are needed to evaluate the underlying model assumptions.

Introduction

A basalt aquifer near Fallon, Nevada, in the Carson Desert Hydrographic Area, is the sole source of water for municipal supply to the City of Fallon, Naval Air Station Fallon, and the Fallon Paiute-Shoshone Tribe (fig. 1). The Carson Desert is the terminus of the Carson River and also receives surface-water flow from the Truckee River through the Truckee Canal (fig. 1). The basalt that forms the basalt aquifer crops out at Rattlesnake Hill, an eroded volcanic cone, about a mile northeast of Fallon. The water-producing part of the basalt is buried beneath sediments deposited by the Carson River and ancient Lake Lahontan to depths of 600 feet near its edges (figs. 2 and 3). In three dimensions, the basalt is a mushroom-shaped body of highly permeable volcanic rock. Viewed from above the aquifer is oval-shaped, about 4 miles wide and 10 miles long (fig. 3).

Pumpage from the basalt aquifer increased from about 1,700 acre-ft/yr in the early 1970's to over 3,000 acre-ft/yr in the late 1990's, causing water levels in the aquifer to decline as much as 12 ft over the same time period (Maurer and Welch, 2001, p. 30). Increased pumpage also is thought to have caused changes in water quality; Maurer and Welch (2001) reported the concentration of dissolved chloride in water pumped from the basalt by Navy and City of Fallon wells has increased from the 1970's to the late 1990's. Although chloride concentrations are still below the drinking-water standard of 250 mg/L, these changes have caused concern over the continued viability of the basalt aquifer as a source of water as development in the area continues. Concentrations of arsenic in the aquifer are about 0.1 mg/L, exceeding the drinking-water standard of 0.01 mg/L (Federal Register, 2001). Arsenic concentrations apparently did not change between the early 1970's and the late 1990's, although changes in analytical and sampling methods could mask actual changes (Maurer and Welch, 2001, p. 10 and 48).

Declining water levels and changing water quality might be mitigated by storing treated surface water in the basalt aquifer for subsequent use. Treated surface water could be injected directly into the basalt aquifer or infiltrated through surface ponds on Rattlesnake Hill. The combined use of ground-water and surface-water resources often is called conjunctive use, and potentially could slow ground-water level declines and decrease chloride and arsenic concentrations. However, study is needed to evaluate the potential for arsenic release from the basaltic rock to the recharged water.

With this objective in mind, in April 2001, the U.S. Geological Survey (USGS), in cooperation with the Fallon Paiute-Shoshone Tribe, began a study to characterize the water quality of the S-Line Canal near Rattlesnake Hill (fig. 3), a likely source for surface water, and to determine the potential for this water to cause arsenic release from the basalt.

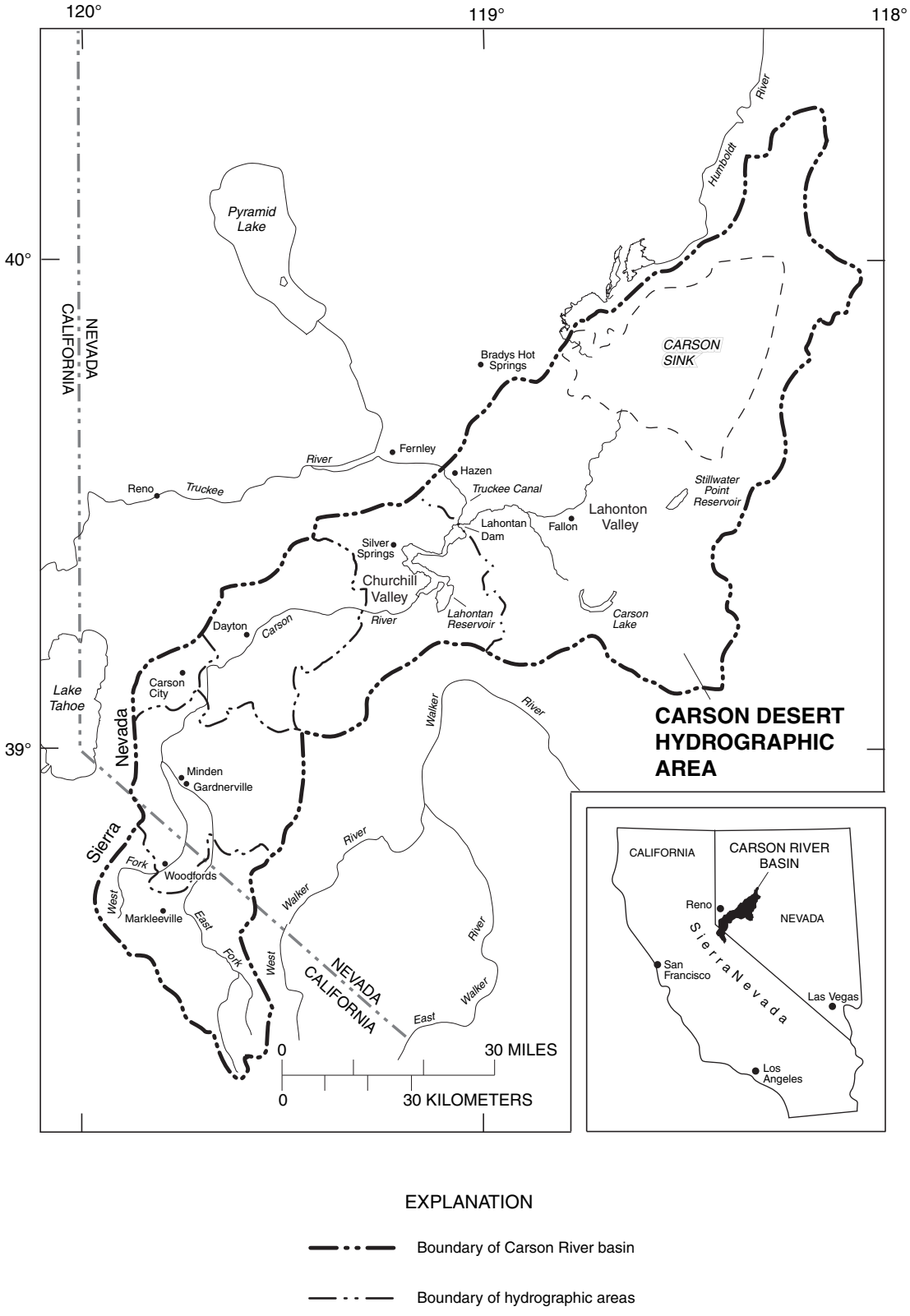

Figure 1. Geographic features of Carson Desert hydrographic area and Carson River basin.

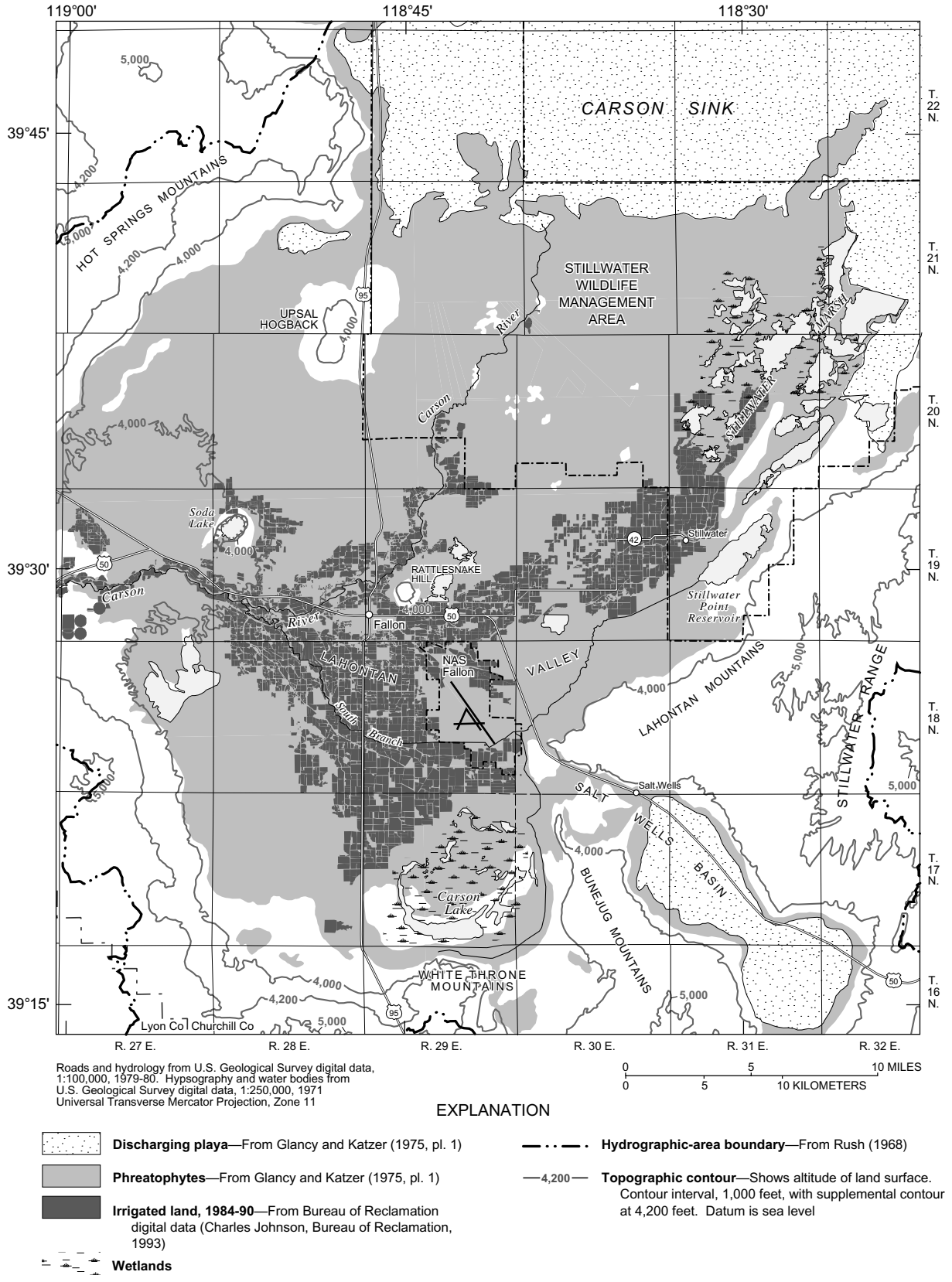

Figure 2. Geographic features of Lahontan Valley and location of irrigated land, phreatophytes, and discharging playas.

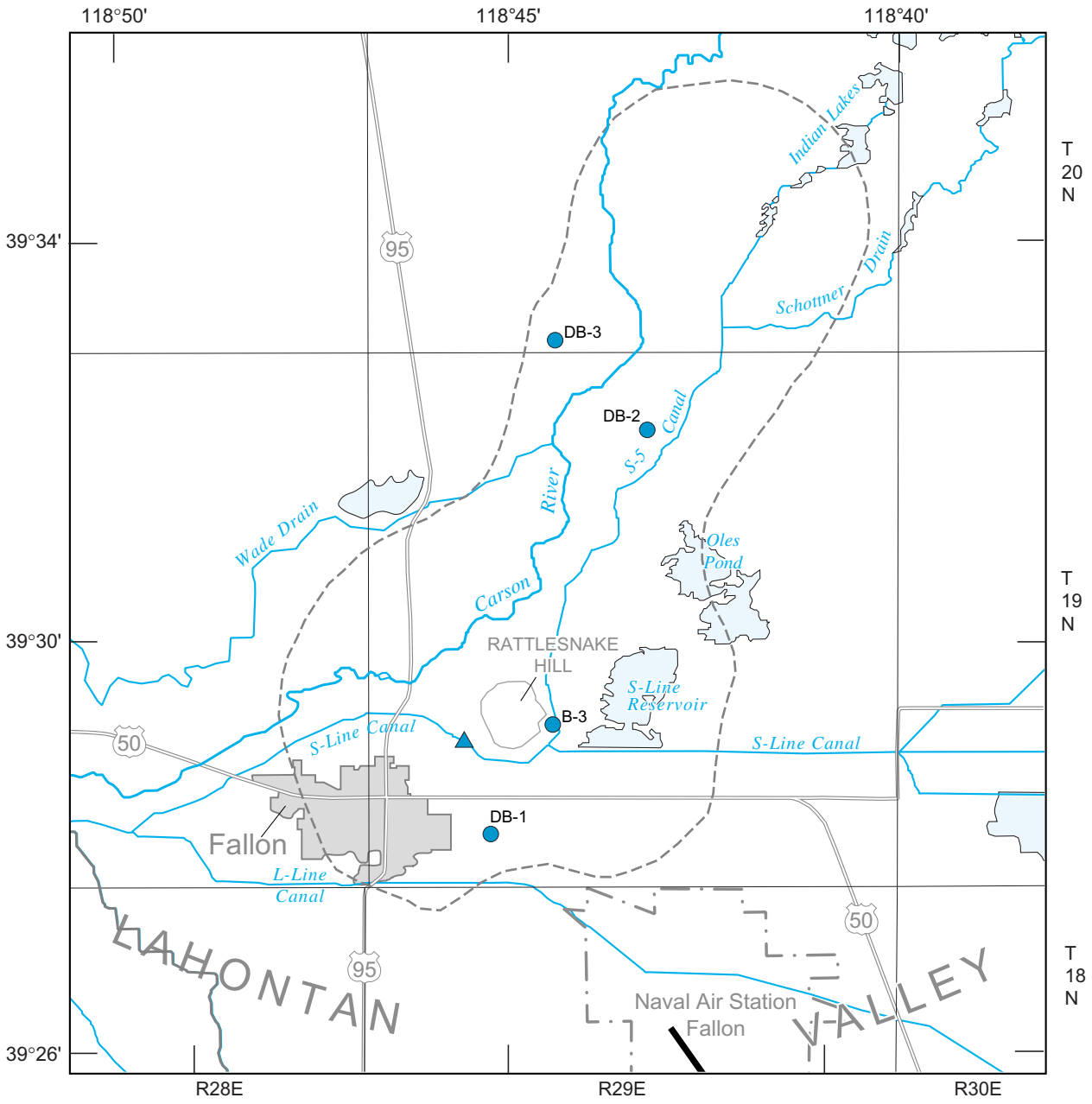

Figure 3. Lateral extent of basalt aquifer and location of wells drilled into basalt aquifer.

Purpose and Scope

The purpose of this report is to present results of water-quality analyses of surface water in the S-Line Canal near Rattlesnake Hill and geochemical analyses of samples of basaltic rock and associated coatings. Results of modeling potential geochemical reactions within the basalt aquifer during recharge also are presented. Nine samples of surface water were obtained from the S-Line Canal from May 2001 through October 2002 and analyzed for major ions, trace metals, nutrients, radioactive constituents, dissolved and total organic carbon, pesticides and polychlorinated biphenyls, dissolved and total mercury, and selected wastewater indicators. Five samples of basaltic rock collected from surface outcrops on Rattlesnake Hill and from cores taken during drilling of the basalt were analyzed for the chemical composition of minerals making up the basalt, and of coatings on fractures and within vesicles of the basalt. Basalt samples also were subjected to chemical extractions to evaluate the cation and anion exchange capacity and the composition of carbonate and iron oxide. Results of the water-quality and rock analyses were used to simulate geochemical reactions that could affect arsenic concentrations using the computer program PHREEQC (Parkhurst and Appelo, 1999).

Acknowledgments

The authors thank Blair Jones and Daniel Webster, USGS, Reston, Virginia, for their X-ray diffraction work; Paul Lechler, University of Nevada, Reno, for whole-rock analyses; Rikkert Vos, BC Research Inc., Vancouver, British Columbia, Canada, for chemical extractions; and Lawrence Feinson, USGS, for simulations using PHREEQC. Richard Sanzalone, USGS, provided valuable insight into the use and interpretation of chemical extractions. Keith Halford, USGS, provided spreadsheet assistance.

Methods Used

Water Sampling Methods

Water samples were collected from S-Line Canal (fig. 3) during 2000–2002 (site 1031221902 in Berris and others, 2003). Samples were collected monthly or bimonthly when the canal was flowing, typically from April-May to about October (see Appendix 1). Water samples were obtained using the equal-width-increment method described by Wilde and Radtke (1998). A DH-81 handheld sampler fitted with a Teflon nozzle and a 1-L bottle was used to obtain water at each vertical in the cross section and these samples were composited into 3-L Teflon bottles. The samples were split into subsamples using an all-Teflon cone splitter described by Capel and Larson (1996). Each subsample was treated with the appropriate preservation method as outlined by Wilde and Radtke (1998). Sample processing was done using techniques described by Wilde and Radtke (1998). Specific conductance and pH were measured on a split of the raw sample. Alkalinity was determined in the field using incremental titration with sulfuric acid on an aliquot of filtered water. Dissolved oxygen and temperature were measured directly in the canal.

Ground-water samples were collected from well B-3 (fig. 3; Appendix 1) located near a potential recharge basin on the eastern flank of Rattlesnake Hill. Well B-3 is a 71-ft deep, 2-in. PVC, monitoring well. The well is screened just below the water table. The basalt aquifer is encountered at 32 ft below land surface at the well, and accordingly, the water quality at well B-3 is believed to be representative of the water beneath the site of a potential recharge basin.

Ground-water samples were collected and processed following protocols described by Wilde and Radtke (1998). Before water samples were collected, the water level in the well was measured, the well was purged of at least three well-bore volumes of water, and field parameters (pH, specific conductance, temperature, and dissolved oxygen) were measured in a flow-through chamber until they were stable (Wilde and Radtke, 1998). An all stainless steel and Teflon pump system was used to obtain water samples from wells. Water samples that required filtration were filtered with in-line 0.45-μm pore-size capsule filters. Whole-water samples were filled directly from the discharge line of the pump. Water samples were preserved following methods outlined in Wilde and Radtke (1998). Alkalinity was determined in the field using incremental titration with sulfuric acid on an aliquot of filtered sample.

Geochemical and Mineralogic Analytical Methods

Water samples were analyzed at the USGS National Water Quality Laboratory in Lakewood, Colorado and the USGS Stable Isotope Laboratory in Reston, Virginia. Major cations and most trace elements were analyzed using inductively coupled plasma mass spectrometry (Fishman, 1993; Fishman and Friedman, 1989; Garbarino, 1999; Struzeski and others, 1996). Arsenic and selenium were analyzed by graphite furnace atomic absorption spectrometry as described by Jones and Garbarino (1999). Nutrient species were analyzed by the methods described in Fishman (1993), Fishman and Friedman (1989), and Patton and Truitt (2000). Pesticides were extracted from the water samples with C-18 solid-phase extraction and analyzed using capillary-column gas chromatography with mass spectrometry (Madsen and others, 2003; Zaugg and others, 1995). Wastewater indicators were analyzed by polystyrene-divinylbenzene solid-phase extraction and capillary-column gas chromatography with mass spectrometry (Zaugg and others, 2002). The stable isotopes of water were determined using methods described by Coplen and others (1991) for hydrogen and those described by Epstein and Mayeda (1953) for oxygen. Gross alpha and beta radioactivity were determined using alpha and beta counting methods described in Thatcher and others (1977).

The mineralogy of the basalt and coatings were determined by X-ray diffraction by Daniel Webster, USGS, Reston, Virginia, and by optical microscopy. Basalt samples and vug-filling material were examined by SEM/EDS (scanning electron microscopy/energy dispersive spectrometry) using a JEOL model 840A with KEVEX EDS/imaging programming. The EDS is capable of qualitative identification of elements having an atomic weight of 12 or greater. Samples were air-dried, mounted on metal tabs, and coated with a thin layer of gold. Images can be taken simultaneously with EDS analyses. Whole rock analyses of cuttings retrieved during drilling of test hole DB-3 (fig. 3) were made under the supervision of Paul Lechler, Nevada Bureau of Mines and Geology, using X-ray fluorescence. Results of the mineralogical examination expand on the work of Lico and Seiler (1994), who provide a description of the mineralogy of cuttings from a well owned by the Fallon Paiute-Shoshone Tribe on the west side of Rattlesnake Hill (fig. 3).

Chemical extraction methods, which also are known as partial solution techniques, have been developed to obtain information about the chemistry of heterogeneous earth materials, such as rocks and soils. Under ideal conditions, sequential extractions can provide information on the association of elements with various minerals within a rock or soil. Reactions involving exchangeable ions, carbonate minerals, and iron oxide are of particular concern in the Fallon area because of potential release of arsenic from rocks and soils into the ground water. Commonly, extraction solutions are applied in order from the least to most chemically aggressive. For instance, a sequence of extractions could attempt to determine solutes that are progressively released by exchange, followed by dissolution of carbonate minerals, organic material, and sulfide minerals. Extractions for organic material and sulfide minerals were not used in this study.

Basalt obtained by drilling and the surface samples taken from rock outcrops were selected for sequential extraction using the methods of Sumner and Miller (1996) and Tessier and others (1979). The extractions were performed in duplicate on samples weighing about 50 g. The samples were approximately ¾-in. by ¾-in. pieces of drill core or outcrop and were not crushed prior to extraction. This size was selected to approximate the actual rock surface area of vesicular and fractured basalt within the aquifer. Details of the analytical steps are presented in Appendix 3.

Physical Setting

Carson River water and diversions from the Truckee River are stored in Lahontan Reservoir and used to irrigate about 56,000 acres of land in Lahontan Valley, the name commonly applied to the irrigated part of the Carson Desert (fig. 2; Maurer and Welch, 1996, p. 4). Irrigated lands form the Carson Division of the Newlands Project, constructed from 1902 to 1915. Canals provide water to agricultural land, including the S-Line and L-Line Canals that flow south and east of Rattlesnake Hill (fig. 3). Surface water not used for irrigation drains north to the Carson Sink, northeast to wetlands of the Stillwater Marsh, and south to the Carson Lake wetlands (fig. 2).

Alfalfa is the main irrigated crop in the valley along with pasture, other forage crops, and some cereal and vegetable crops. Cottonwood is abundant near homes and ranches in the irrigated part of the valley, willows line many of the canals, and cattails are present in many drains. Except for the Carson Sink, which is largely barren, non-irrigated areas are sparsely vegetated with greasewood, rabbitbrush, saltgrass, and marsh grasses.

The city of Fallon is the major and growing population center in the area. The population of Fallon has increased from about 3,000 in the early 1970's (Glancy, 1986, p. 27) to 8,800 in 2000 with about 15,000 additional people living in the surrounding unincorporated parts of the county (http://factfinder.census.gov). Agriculture is a major economic base in the area, along with employment at the Naval Air Station Fallon.

The floor of Lahontan Valley is a relatively flat plain, sloping from about 3,960 ft above sea level near Fallon to about 3,870 ft near the Carson Sink (fig. 2). Several low-lying mountain ranges rising to about 5,500 ft in altitude surround the valley on the north, south, and west. The Stillwater Range, rising to 8,800 ft in altitude, bounds the valley on the east. Lahontan Valley is in the rain shadow of the Sierra Nevada and received an average 5.3 in. of annual precipitation from 1960 to 1991 (Owenby and Ezell, 1992, p. 15). Summer temperatures reach an average maximum of about 90°F in July and August, and average minimum temperatures are about 18°F in December and January (Owenby and Ezell, 1992, p. 11). Open-water evaporation is about 5 ft/yr (Bureau of Reclamation, 1987, p. 1–7).

Hydrogeologic Setting

Recent Geologic History

During the Pleistocene Epoch [about two million years before present (Ma) to ten thousand years before present (ka)], lakes formed in the Carson Desert, expanded, and shrank to complete dryness several times under the influence of changing glacial climates (Axelrod, 1956; Morrison, 1964). During high stands, the lakes coalesced to form ancient Lake Lahontan having a depth of more than 500 ft near Fallon (Davis, 1978, p. 2; Morrison, 1991, p. 288). High stands of Lake Lahontan were from 1.2 Ma to 850 ka, 650 to 600 ka, 400 to 130 ka, and 25 to 10 ka (Benson, 1991; Benson and others, 1990, p. 241). During high stands of Lake Lahontan, thick clay beds were deposited in the deeper parts of Lake Lahontan, deltas were formed on the western side of the valley where the Carson River entered the lake, and sand and gravel beaches

and bars were formed by wave action along the shorelines (Morrison, 1964, p. 28–71). During interglacial periods when Lake Lahontan was dry, large sand-dune and sand-sheet complexes covered much of the valley floor and the Carson River meandered across the valley floor forming river channels which are now buried. As lake levels rose and fell, these depositional environments moved back and forth across the valley floor, creating a complex mixture of Quaternary sediments, locally reaching a thickness greater than 2,500 ft (Maurer and Welch, 1996, p. 11).

Also during the Pleistocene Epoch, isolated volcanic activity produced Rattlesnake Hill, an eroded volcanic cone about 1 mi in diameter and about 200 ft high with a shallow crater at the center (Morrison, 1964, p. 23). The cone was formed by repeated basalt flows, issuing radially from Rattlesnake Hill for 2 to 7 mi. (fig. 2) to produce the mushroom-shape basalt aquifer described by Glancy (1986, p. 14). A sample of the basalt from the high point of Rattlesnake Hill was dated by whole-rock potassium-argon analysis to be 1.03 ± 0.05 Ma (Evans, 1980, p. 20), and argon-argon dates from the upper surface of the basalt near its western and southern extent range from 2.5 ± 0.3 Ma to 1.3 ± 0.2 Ma (Maurer and Welch, 2001, p. 16). Stratigraphic evidence shows that the basalt is older than the early high stands of Lake Lahontan (Morrison, 1964, p. 23) which indicates that the basalt was present during the entire history of Lake Lahontan.

Holocene Epoch deposits in the Carson Desert (less than 10 ka) are eolian, alluvial, fluvial, deltaic, and shallow-lake sediments deposited after the last high stand of Lake Lahontan. An extremely dry, windy period followed the last high lake stand from 7 to 4 ka, and shallow lakes were formed in the Carson Desert during the last 5 to 4 ka (Davis, 1978; Morrison, 1964, p. 8). The last of the shallow lakes dried up just before non-native Americans entered the area in the 1800's (Davis, 1978, p. 8).

Description of Aquifers

The basalt aquifer was first described in detail by Glancy (1986), who also defined three basin-fill aquifers that envelope the basalt. Glancy (1986, p. 41) defined a shallow aquifer extending from the water table, generally 5 to 10 ft below land surface, to a depth of 50 ft below land surface. Below the shallow aquifer, an intermediate aquifer extends to depths of 500 to 1,000 ft, the approximate range of sediments bearing fresh water near the basalt aquifer (Glancy, 1986, p. 51). The intermediate aquifer contains fresh water beneath much of the southern Carson Desert. A deep aquifer extends beneath the intermediate aquifer to depths of several thousand feet, and is thought to be mainly non-potable because of a high dissolved-solids content (Glancy, 1986, p. 51 and 60).

Glancy (1986) delineated the extent of the basalt aquifer using lithologic descriptions from driller's logs and surface electrical resistivity soundings. He described it as an asymmetrical, mushroom-shaped body of basalt exposed at Rattlesnake Hill with the bulk of the basalt enveloped by the sedimentary aquifers (Glancy, 1986, p. 13–14). Drillers' logs show the basalt is 400–600 ft below land surface near its southwestern extent about 2 mi southwest of Rattlesnake Hill, and about 200–300 ft below land surface near its northeastern extent 5–7 mi northeast of Rattlesnake Hill (fig. 4). Electrical resistivity data indicates that at depths greater than 1,000 ft below land surface, the basalt narrows to a thin neck approximately centered beneath Rattlesnake Hill. Seismic-reflection profiles presented by Maurer and Welch (2001, pgs.16 and 19) largely confirm the lateral extent of the basalt described by Glancy (1986). The seismic profiles indicate the presence of a secondary vent in the northern part of the basalt that is not exposed at land surface (fig. 4).

Exposed basalt consists of loosely consolidated scoriaceous cinders near the top of Rattlesnake Hill (fig. 5) and vesicular flows along the flanks of Rattlesnake Hill (fig. 6). Recent drilling at test hole DB-1, near the southern extent of the aquifer (fig. 3), penetrated about 300 ft of very porous and fractured basalt alternating with more massive zones (Maurer, 2002). Core material from test hole DB-1 (fig. 7) is similar in appearance to cuttings from other test wells drilled near the southern half of basalt aquifer and to the vesicular flows along the flanks of Rattlesnake Hill. To the north, test hole DB-2 penetrated about 340 ft of low permeability, brecciated and massive basalt (Maurer, 2002).

Water quality in the basalt aquifer generally is uniform over its lateral extent and is suspected to be a blend of fresh water and water with a higher dissolved solids content. The observed increase in dissolved chloride over the past 30 years indicates that more saline water may be migrating into the basalt aquifer. Maurer and Welch (2001, p. 48) suggest the source of the more saline water may be near the southern edge of the basalt from depths greater than 300 ft below land surface. Recent drilling (Maurer, 2002) shows that water quality within the basalt, near its southern extent, is fairly uniform through its entire thickness of about 290 ft, and that ground water in the underlying intermediate aquifer contains chloride concentrations of nearly 2,000 mg/L. Thus, the underlying aquifer could be a source for the increasing chloride concentrations. Maurer and Welch (2001, p. 42 and 43) suggest the basalt is recharged by a mixture of water from the shallow aquifer near Rattlesnake Hill, water from the intermediate aquifer on the southwest, west, and northwest side of the basalt, and more saline water from depths greater than 300 ft below land surface.

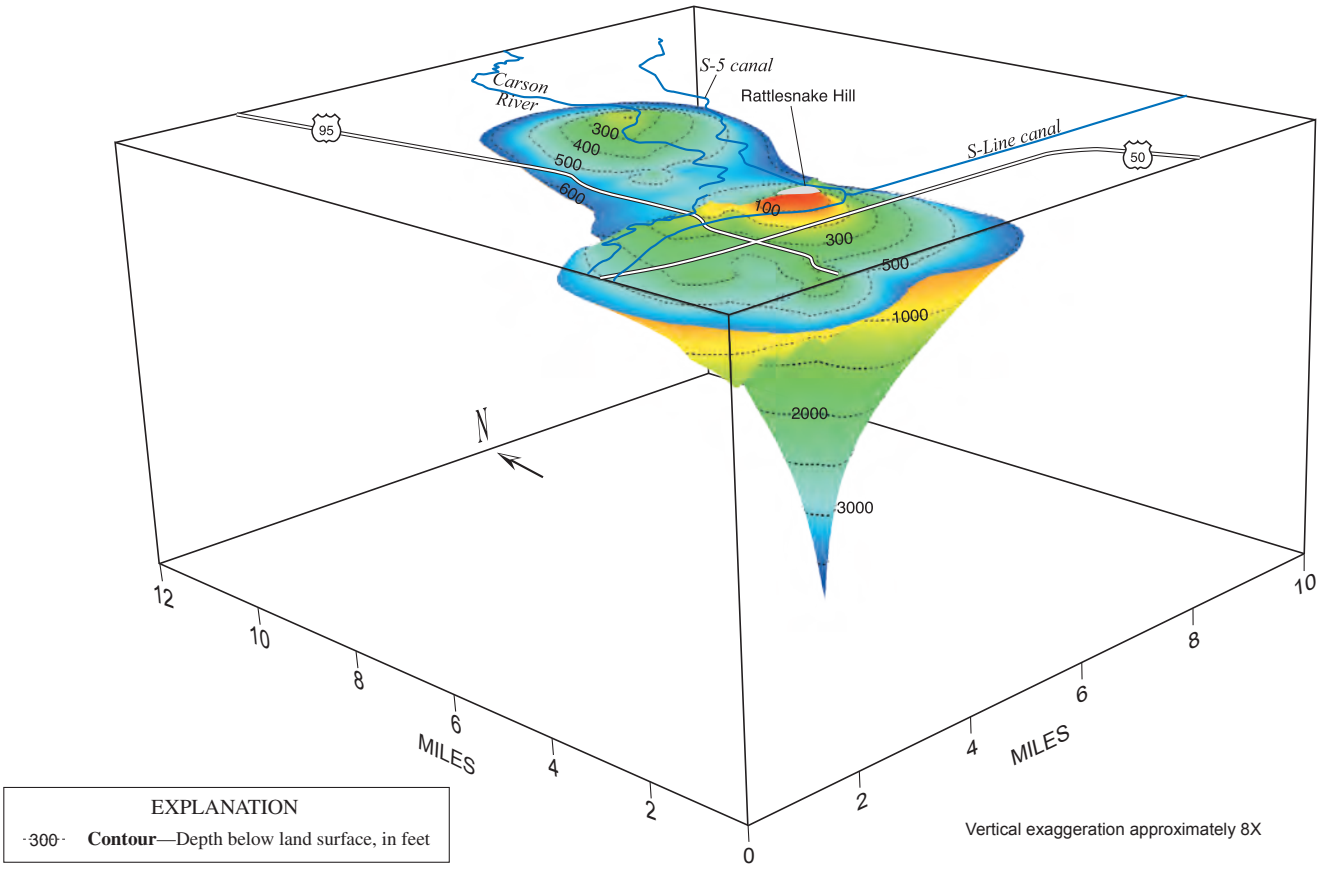

Figure 4. Oblique view of basalt aquifer, looking toward northeast. Modified from figure 8B in Maurer and Welch (2001).

Figure 5. Scoriaceous cinders near the top of Rattlesnake Hill. Bottle is 10-inches high, used for scale.

Figure 6. Vesicular basalt flows on the southern flank of Rattlesnake Hill. Wallet is used for scale.

Figure 7. Fractured, vesicular basalt from well DB-1 recovered from a depth of 441–442 ft below land surface.

Chemistry and Mineralogy of the Basalt Aquifer

The mineralogy of unweathered basalt is dominated by fine-grained plagioclase and augite, as determined by X-ray diffraction. The plagioclase and augite are partially altered to illite and chlorite. Optical microscopy reveal a classic olivine basalt: plagioclase, clinopyroxene, olivine, and opaque minerals in a fine-grained groundmass. Olivine and iron-bearing minerals (ilmenite or magnetite) are present in minor amounts (Lico and Seiler, 1994). Plagioclase occurs as finer groundmass and as somewhat larger phenocrysts. The plagioclase composition varies over the relatively narrow range of An50-55 (labradorite to andesine-labradorite). Plagioclase exhibits both normal concentric zoning (more calcic cores) and oscillatory zoning. Clinopyroxenes are smaller and are typically subhedral groundmass materials, with few coarse phenocrysts. EDS analyses of the clinopyroxenes indicate that they are diopsidic because they contain very low aluminum and iron and abundant calcium and magnesium. Olivine typically forms larger grains, is subhedral, and colorless. EDS analyses of the olivine indicates a forsteritic composition because the olivine contains relatively small amounts of iron. EDS analyses of the opaque minerals indicate that most are ilmenitic (Fe-rich titanium oxides), but some contain significant chromium. The opaque minerals are not significantly magnetic.

Even though mineralogy of the basalts is consistent throughout the sections, they fall into two subtypes based on relative plagioclase and opaque mineral contents. Type 1 is defined here as containing significantly less plagioclase and more opaque minerals than type 2. Typical images of both types are shown in figures 8 and 9. Comparison of these figures demonstrates the higher plagioclase and lower opaque mineral content of type 2 compared to type 1 basalt.

Despite a difference in plagioclase and opaque mineral concentrations between the two basalt types, plagioclase composition is very similar in both types, indicating they originated from similar, if not the same, parent magma. Several samples of both basalts are visibly argillized and chloritic. The high Loss-On-Ignition (LOI; table 1) indicates that these samples were weathered and altered, and probably include zeolite and clay materials. This alteration also may explain why the aluminum and potassium content of these samples is significantly higher than in most basalts. Conversely, the magnesium content is significantly lower than in most basalts. The low titanium values compared to typical basalts (table 1), and the olivine character of these samples indicates that they are a mid-ocean ridge type basalt. Arsenic concentrations for four basalt samples recovered from depths of 399–730 ft below land surface ranged from 0.66 to 1.2 mg/kg (table 1).

Table 1. Bulk chemical composition of the basalt aquifer encountered at test hole DB-1.

[Symbol: --, not available]

Parameter, in weight percent except as noted	Sample depth, in feet				Typical basalt[1]	
	390 to 399	433	482	730	Mean	Standard deviation
SiO_2	49.5	49.2	50.4	51.2	50.06	3.65
TiO_2	1.92	1.54	1.87	1.66	1.86	1.1
Al_2O_3	16.9	17.4	18	17.4	15.99	2.58
Fe, as Fe_2O_3	8.93	7.01	8.79	8.15	11.38	--[2]
MnO	.17	.11	.14	.017	--	--
MgO	5.42	3.05	3.28	4.69	6.96	2.97
CaO	8.53	9.78	7.93	8.55	9.66	1.91
Na_2O	3.33	3.68	3.94	3.27	2.97	0.91
K_2O	2.17	2.62	2.13	2.19	1.12	0.75
P_2O_5	.78	.7	.065	0.71	--	--
Loss On Ignition	2.26	4.38	2.26	2.26	--	--
Total	100.57	99.47	98.805	100.097	100	--
As[3]	.66	1.00	.8	1.17	--	--

[1] Values are based on 3,594 analyses (Le Maitre, 1976).

[2] Le Maitre (1976) presents standard deviations for Fe_2O_3 and FeO (2.17 and 2.5, respectively) individually rather than for total iron.

[3] Concentrations in mg/kg.

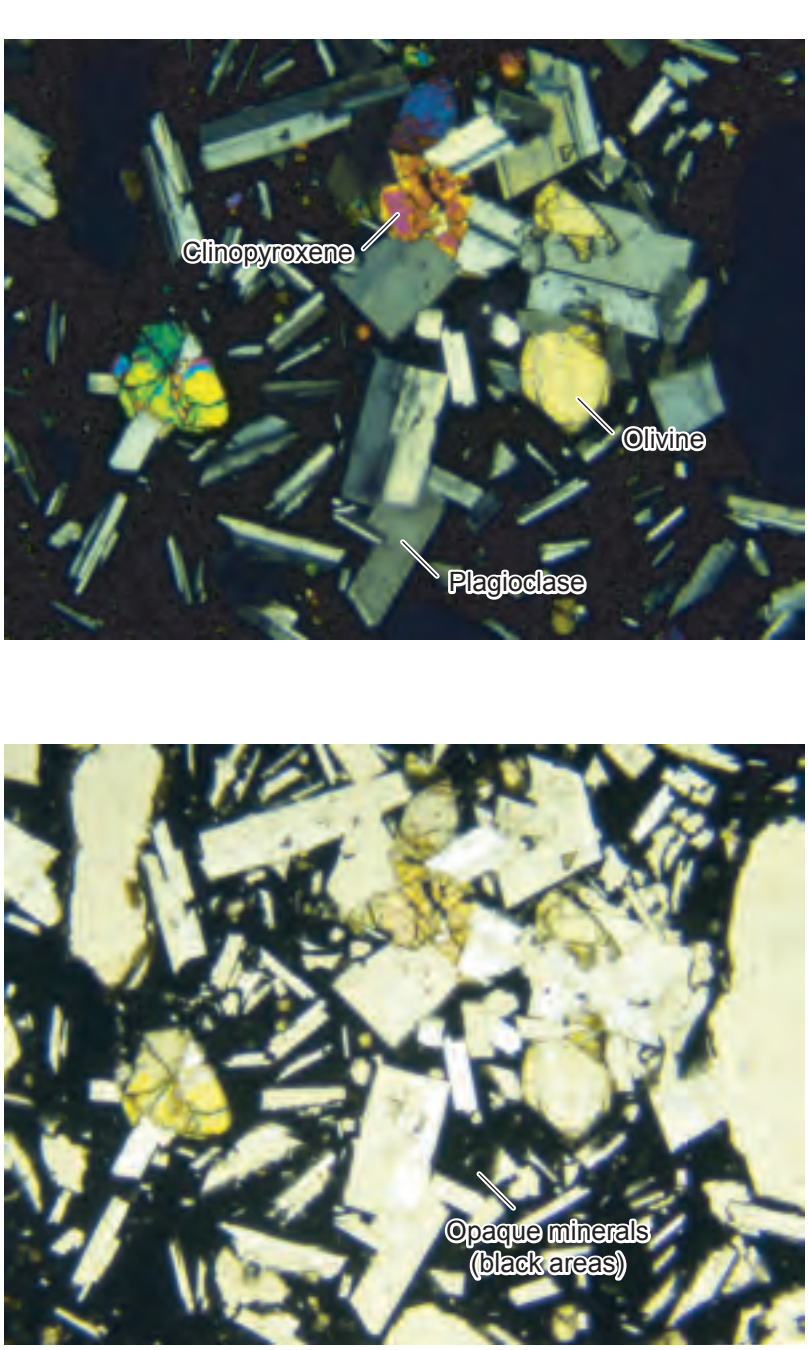

Figure 8. Optical microscope micrograph of Type 1 basalt from well DB-1 at 545 ft with (***A***) crossed polarizers and (***B***) uncrossed polarizers. Field of view is 6 mm. These images show the bimodal size distribution of plagioclase, and typical size and form of olivine and clinopyroxene grains. The uncrossed view plainly shows the opaque mineral content.

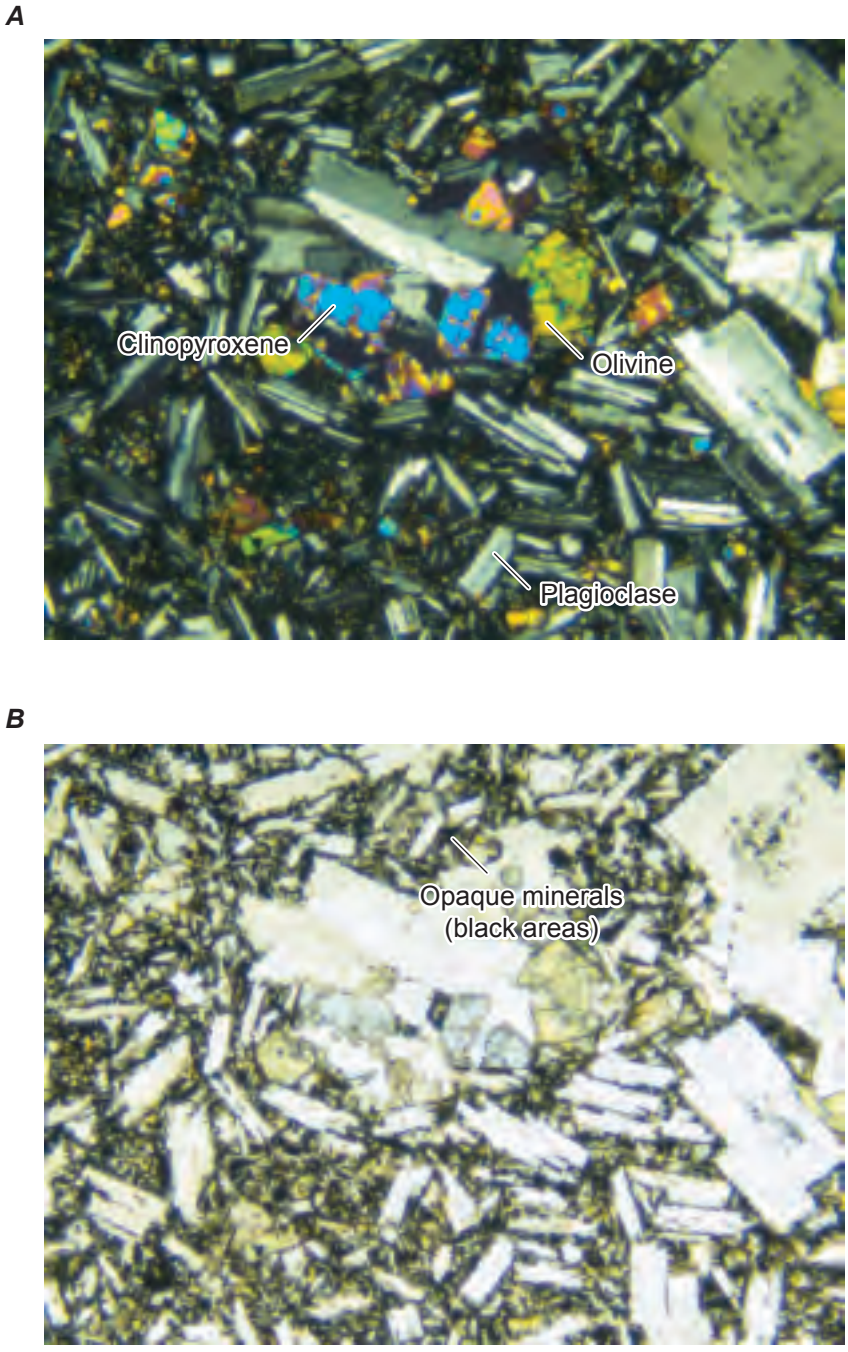

Figure 9. Optical microscope micrograph of Type 2 basalt from well DB-1 at 441 ft with (***A***) crossed polarizers and (***B***) uncrossed polarizers. Field of view is 6 mm. These photographs are taken at the same magnification of those in figure 8 and clearly show the higher plagioclase and lower opaque mineral content of Type 2 basalt relative to Type 1.

X-ray diffraction and SEM/EDS analysis of material from sites DB-1 and B-7 (fig. 10 and 11) show that fracture surfaces and vesicles (vugs) in the basalt contain coatings that include phillipsite, dolomite, calcite, clay minerals, and iron oxide. These minerals are important from the standpoint of water chemistry because they can dissolve or have easily exchangeable ions, which can alter the chemical quality of the injected water. For example, phillipsite is a zeolite with cation-exchange sites that can react with injected water. Vug-filling materials in samples from other sites were very similar to the materials shown in figure 10 and no other mineral phases were identified.

Sequential chemical extractions of basalt aquifer material indicates the presence of exchangeable cations and anions, calcite, and iron oxide (table 2). The presence of calcite and exchangeable cations is important because calcite dissolution and cation exchange can alter the water chemistry. The presence of iron oxide is particularly important because it can adsorb or release arsenic. The results of the chemical extractions can be used in geochemical models to predict the behavior of arsenic during recharge and withdrawal of water from the basalt aquifer.

Characterization of Surface Water in the S-Line Canal

Analytical results for surface-water samples from the S-Line Canal are presented in Appendixes 1 and 2. Water used for irrigation and maintenance of wildlife areas in Lahontan Valley originates as runoff from the Sierra Nevada. Water from the Carson River and water imported from the Truckee River via the Truckee Canal are stored in Lahontan Reservoir. The S-Line Canal is one of the principal delivery canals in the extensive network of canals that transports water through Lahontan Valley. During a typical year, water released from Lahontan Reservoir maintains flow in the S-Line Canal from April to October.

Water in the S-Line Canal (Appendix 1) is a Na-Ca-HCO_3 type water, with pH ranging from 7.7 to 8.2, and total-dissolved solids concentrations of about 195 mg/L. Sulfate concentrations have a narrow range of about 30–48 mg/L. Nitrogen and phosphorus concentrations generally are low, none exceeding 0.45 mg/L as N or 0.2 mg/L as P.

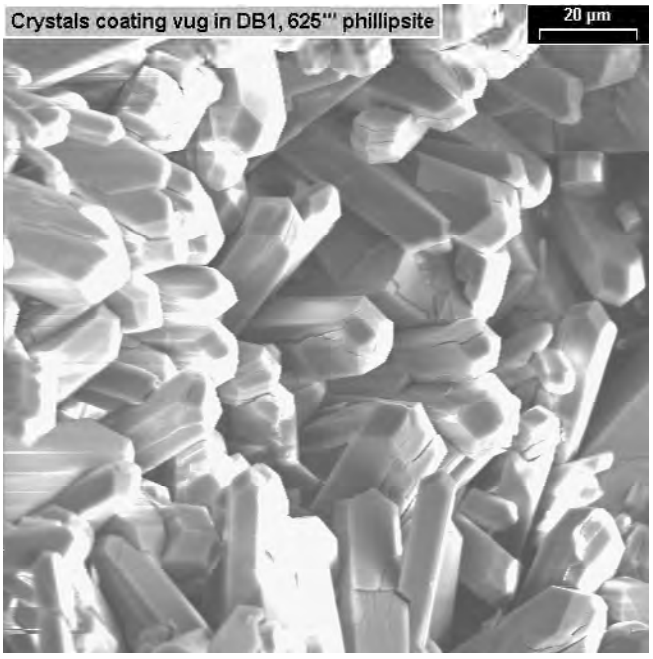

Figure 10. Scanning electron microscope micrograph of vug-filling material from well DB-1 at a depth of 625 ft showing phillipsite. Phillipsite was identified by the occurrence, morphology, and EDS compositional analyses which identified abundant silica, aluminum, potassium, and sodium with no other cations present.

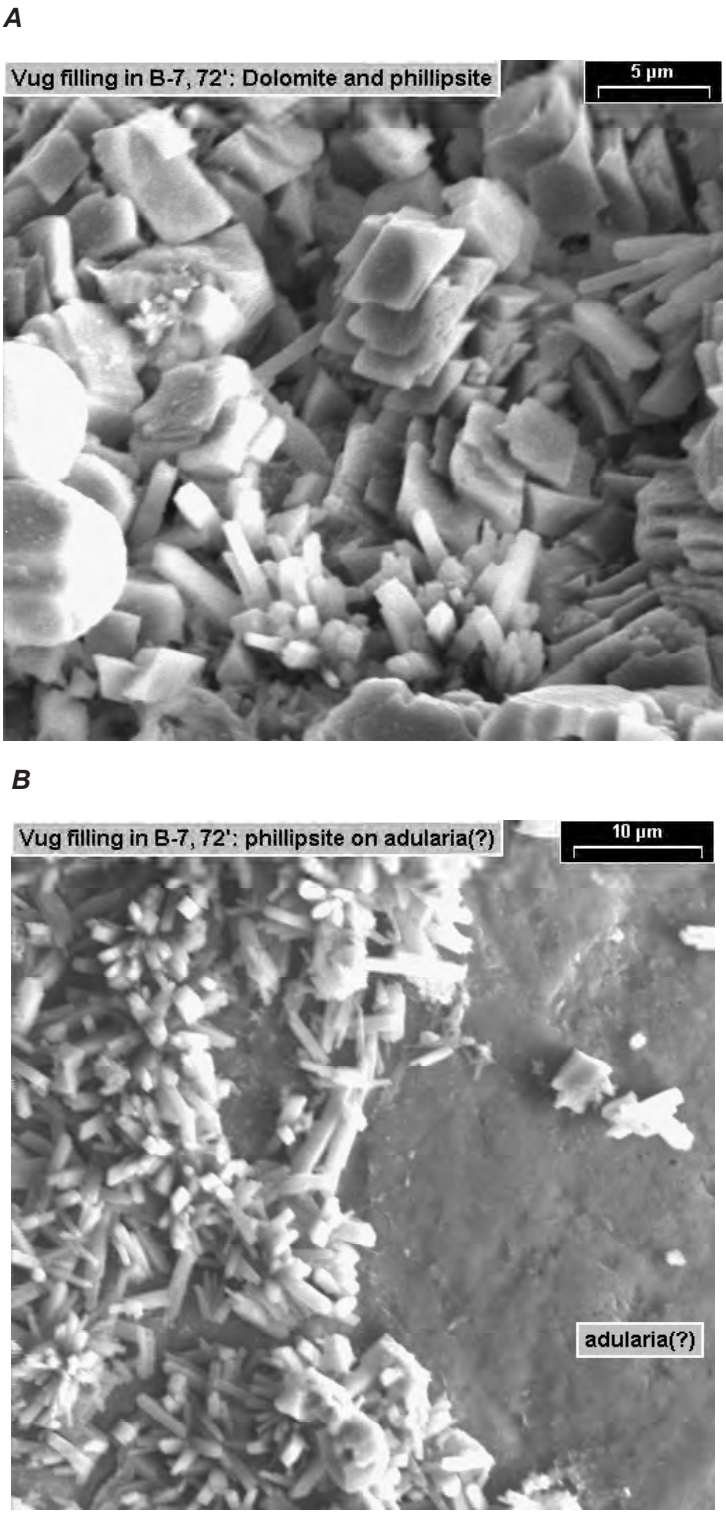

Figure 11. Scanning electron microscope micrograph of vug-filling material from well B-7 at a depth of 72 ft showing (***A***) dolomite rhomboids above phillipsite rhomboids and (***B***) phillipsite prisms on surface of adularia. Dolomite identified by morphology and EDS analyses, which identified calcium. Adularia identified by its vug-filling secondary occurrence, and EDS analyses which identified potassium, silica, and aluminum.

Table 2A. Concentration of elements released from basalt rock samples following cation exchange using ammonium chloride.

[Concentrations are in mg/kg, milligram per kilogram]

Sample identifier[1]	Calcium	Potassium	Magnesium
DB-1 442A	184	135	37
DB-1 442B	393	155	46
RSHCA	1,580	303	78
RSHCB	2,190	227	124
RSHO	173	16.5	4.1

Table 2B. Concentration of elements released from basalt rock samples following anion exchange using potassium nitrate.

[Concentrations are in mg/kg, milligrams per kilogram]

Sample identifier[1]	Chloride	Phosphorus	Arsenic
DB-1 442A	11.4	36	0.08
DB-1 442B	6.7	37.1	0.08
RSHCA	35.3	33.9	0.08
RSHCB	15.4	36.6	0.04
RSHO	7.4	36.2	0.04

Table 2C. Concentrations of elements released from basalt rock samples following extraction of carbonate minerals by sodium acetate and acetic acid.

[Concentrations are in mg/kg, milligram per kilogram. Symbol: <, less than]

Sample identifier[1]	Aluminum	Arsenic	Calcium	Iron	Potassium	Magnesium	Manganese	Phosphorus	Lead	Silica	Sulfate
DB-1 442A	<4	4	992	35.9	1,620	81.6	2.4	11	0.69	153	2,280
DB-1 442B	<4	3.2	4,620	28	2,150	167	16.7	20.1	11.2	187	3,930
RSHCA	42.7	2.3	1,770	26.4	5,160	89.3	5	286	1.8	241	3,570
RSHCB	34.3	2.7	4,780	20.2	4,780	373	12	236	32.2	343	3,990
RSHO	<4	1.8	742	26.4	618	8.2	0.41	27.2	<.4	154	3,170

Table 2D. Concentration of elements released from basalt rock samples following extraction of iron and manganese oxides by hydroxylamine hydrochloride and acetic acid.

[Concentrations are in mg/kg, milligram per kilogram]

Sample identifier[1]	Aluminum	Arsenic	Calcium	Iron	Potassium	Magnesium	Manganese	Phosphorus	Silica	Sulfate
DB-1 442A	71.4	0.2	1,070	103	163	153	29.6	144	223	20.4
DB-1 442B	157	0.42	3,060	167	209	251	50.2	162	403	20.9
RSHCA	544	1.7	2,170	112	272	214	88.3	816	482	214
RSHCB	311	0.97	2,200	91.2	96.6	708	103	616	622	193
RSHO	72.1	0.82	1,100	99.9	61.8	61.8	18.5	547	220	61.8

[1] Sample identifiers: RSHCA, RSHCB, RSHO represent Rattlesnake Hill cinder sample A, B, and vesicular outcrop sample, respectively. DB-1 442A and 442B are basalt core samples from a depth of 442 feet below land surface from well DB-1.

Trace-element concentrations and radionuclide activities generally were low and, except for arsenic, did not exceed drinking-water standards. For arsenic, all but one sample exceeded the 10 µg/L Nevada drinking-water standard. The one sample with a low arsenic concentration (1.5 µg/L) was collected in May 2001 (fig. 12) when the flow in the Carson River below Lahontan Reservoir was 790 ft^3/s. These limited data indicate that diverting flow from the S-Line Canal during high flow could minimize the arsenic concentrations in water from the basalt aquifer. Chloride concentrations in the canal were less than 22 mg/L in all the samples collected during this study (Appendix 1), compared with average chloride concentrations in the basalt aquifer that exceed 100 mg/L (Appendix 1 in Maurer and Welch, 2001). Dissolved organic carbon (DOC) concentrations ranged from 2.5 to 5.8 mg/L in the six water samples analyzed for carbon. DOC concentrations in water used for artificial recharge are important because DOC reacts with chlorine to form carcinogenic disinfection-by-products and because metabolism of DOC by bacteria can indirectly mobilize arsenic in an aquifer. DOC concentrations are lowest during spring runoff (Appendix 1), indicating that artificial recharge using water during high flow in the Carson River would have the additional benefit of minimizing the DOC content.

Analyses of water samples for pesticides and other anthropogenic organic compounds show very little contamination of S-Line Canal water with these chemicals. A few pesticides (Atrazine, EPTC, Prometon, and Simizine) were detected at very low levels (<0.01 µg/L) in the water samples but were not common (Appendix 2). Several consumer chemicals, including Bisphenol A, caffeine, cholesterol, and DEET, were detected at very low concentrations, indicating the presence of wastewater in the canal water.

Geochemical Modeling of Recharge

Modeling Approach

Artificial recharge of the basalt aquifer with surface water could mitigate declining water levels and increasing chloride concentrations. However, the chemistry of the surface water could change following recharge, which raises the concern that arsenic may exceed standards in recovered ground water. Ground water in the basalt aquifer has a high pH (Appendix 1), which is characteristic of high-arsenic ground water elsewhere in the United States (Welch and others, 2000). Because high pH values can promote arsenic desorption (Stollenwerk, 2003), reactions that increase the pH of recharged water could increase the arsenic concentrations. An overall reaction that could increase the pH involves cation exchange and calcite dissolution as indicated by the following reaction:

$$CaCO_3 + Na_2\text{-}X + H_2O \leftrightarrow 2\ Na^+ + HCO_3^- + Ca\text{-}X + OH^- \quad (1)$$

Where -*X* represents exchange sites.

The relatively low calcium and magnesium concentrations compared to the sodium concentration in the basalt aquifer are consistent with this exchange reaction.

Calcite containing phosphorus and arsenic has been identified in the basalt aquifer (as indicated by the chemical extraction data in table 2C). Dissolution of calcite in the basalt could directly lead to higher arsenic concentrations by freeing adsorbed arsenic. Welch and others (2003), suggest that dissolution of calcite present in the basalt aquifer results in an increase in aqueous phosphorus. Because phosphate and arsenic compete for adsorption sites on a variety of adsorbants (Stollenwerk, 2003), phosphate released from the calcite may result in higher arsenic concentrations by competitively inhibiting adsorption of the arsenic.

Geochemical reactions that may result from recharge of water from S-Line Canal were simulated using the computer program PHREEQC (Parkhurst and Appelo, 1999), which has been widely used for modeling chemical reactions. Of particular importance for the recharge simulations is the capability of PHREEQC to include adsorption, precipitation, and dissolution reactions along with transport of the water. Modeling adsorption of arsenic requires knowledge of the amount and chemical character of the adsorbent in the aquifer. One common and important adsorbent in aquifers is iron oxide, particularly in ground water containing dissolved oxygen (Welch and others, 2000). The modeling presented below only includes iron oxide because it is present in the basalt aquifer and an internally consistent set of adsorption constants is available for arsenic and other potentially competing ions. The exclusion of other phases that could contribute arsenic to recharged water could lead to an underestimate of the potential for arsenic release.

Surface complexation modeling requires that the site density, the specific area of the surface, and the mass of the adsorbant be specified. Following the approach of Dzombak and Morel (1990), a site density of 0.2 mol/mol and a surface area of 600 m^2/g were used in the adsorption model for iron oxide. These values are applicable for hydrous ferric oxide (HFO), which may overestimate the surface area and site density for a system like the basalt aquifer. Extracted arsenic and iron concentrations, along with values for porosity and density (table 3), were used to estimate the iron oxide content and adsorbed arsenic associated with sampled ground water. Following the approach of Welch and Lico (1998), the laboratory values for extracted arsenic and iron were converted to mol/L of water by using the following general equations:

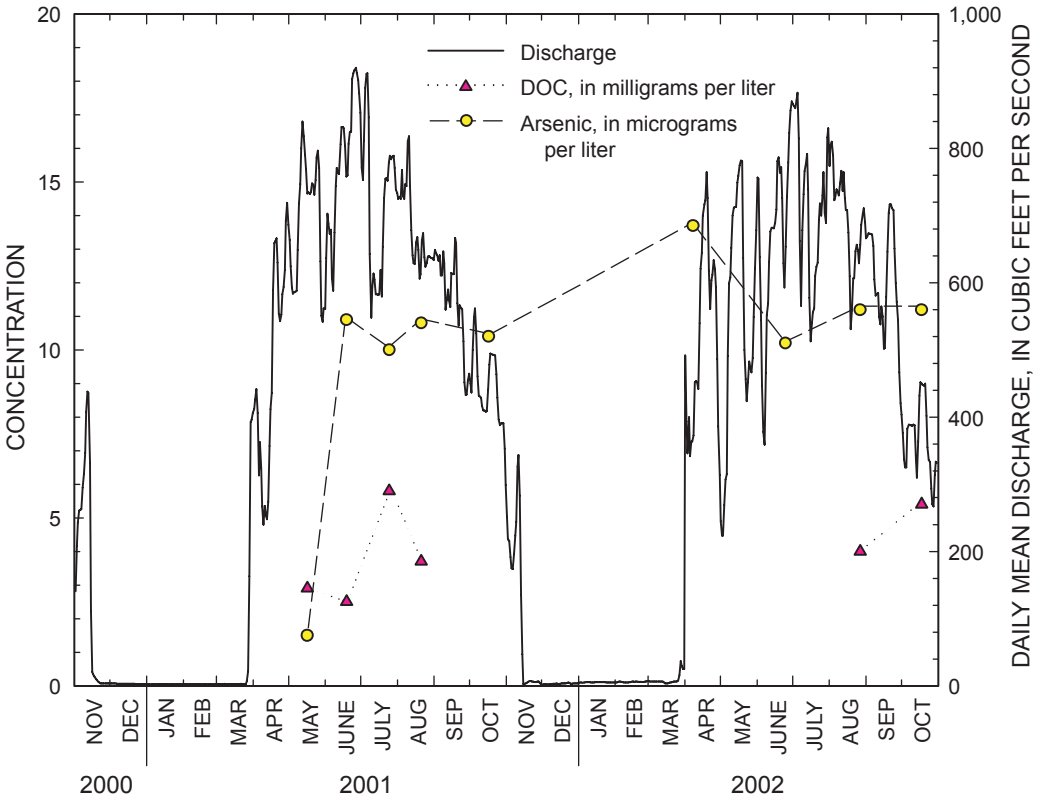

Figure 12. Graph showing arsenic and dissolved organic carbon (DOC) concentrations in S-Line Canal and daily mean flow in the Carson River below Lahontan Reservoir.

$$G = M \times D \times (1-\Phi) \times (1000\ cm^3/L) \times (10^{-6}\ g/\mu g) / (\Phi)$$

and $C = G/W$

Where G = concentration, in g/L

M = mass of arsenic or iron extracted, in µg/g of aquifer material

D = aquifer material density, in g/cm^3

Φ = porosity, dimensionless

C = concentration, in mol/L

W = gram-formula weight of arsenic (74.92 g/mol) or iron (55.85 g/mol)

Competitive adsorption in the simulations uses the 'best fit' models for iron oxide from Dzombak and Morel (1990). More recently, the adsorption of carbonate on iron oxide, both HFO (Appelo and others, 2002) and goethite (Van Geen and others, 1994), has been discussed. The effect of carbonate adsorption on arsenic concentrations was included in the modeling using the adsorption parameters in table 4.

Table 3. Mean bulk density and porosity of basalt samples (Brian Andraski, USGS, 2003, written commun.)

[Abbreviation: g/cm^3, grams per cubic centimeter]

Sample type	Number of samples	Average bulk density (g/cm^3)	Average porosity
Surface outcrop, cinders	2	1.14	0.48
Surface outcrop, flow	2	2.52	.09
Vesicular basalt	4	2.25	.16

Table 4. Surface complexation constants for carbonate adsorption on ferrihydrite. Data from Appelo and others (2002)..

Reaction	Log K
$Hfo\_wOH + CO_3^{2-} + H^+ = Hfo\_wOCO_2^- + H_2O$	12.78 ± 0.48
$Hfo\_wOH + CO_3^{2-} + 2H^+ = Hfo\_wOCO_2^- H + H_2O$	20.37 ± 0.20

Model Scenarios and Limitations

Surface water can be injected directly into ground water through wells or recharged through the unsaturated zone beneath infiltration basins. Simulation of chemical reactions during direct injection and basin spreading are termed 'well-injection' and 'basin-infiltration' models, respectively. Both models considered only advective, or plug flow; that is, dispersion and mixing were not considered. Chemical equilibrium was assumed during each reaction step. The well-injection model consists of reacting water with the basalt aquifer as summarized in table 5. The basalt aquifer was discretized into 10 reaction cells in the saturated zone. The surfaces of the aquifer material prior to injection was assumed to be in chemical equilibrium with basalt-aquifer water. The surfaces were subsequently equilibrated with the recharge water. Withdrawal then was simulated by changing the flow direction and the invading basalt-aquifer water was equilibrated with the chemically altered surfaces of the aquifer material.

The basin-infiltration model added two reaction cells to the well-injection model to simulate initial reactions in the unsaturated zone prior to reactions in the saturated zone (table 5). The first reaction cell simulated reactions with the surface cinder and the second simulated reactions with the vesicular basalt. Simulation of chemical reactions during injection and withdrawal in the saturated zone used the same approach as described for the well-injection model.

The ability of any numerical model to accurately simulate the outcome of a process such as the chemistry resulting from artificial recharge is limited for a variety of reasons. These limitations fall into three broad categories. The first involves formulation of the underlying mathematical approaches for simulation of chemical and physical processes. The second involves the adequacy and applicability of the information required to perform a simulation. The third involves how closely a modeled scenario and the actual recharge approach correspond. These limitations are discussed in turn.

The PHREEQC computer code includes an aqueous model that calculates the chemical activities of the aqueous species. The underlying mathematical approach and thermodynamic data used for the aqueous model are considered fully adequate for the simulations. Ground water with high iron and organic carbon concentrations could be important if organic-rich water were recharged and produced because interaction between arsenic (V) and organic matter can affect aqueous arsenic activities (Redman and others, 2002). The PHREEQC database does not account for this phenomenon. This interaction only appears to be important in water with high iron concentrations (>600 mg/L); thus, this interaction is not expected to be important for the simulations discussed here.

Adsorption of arsenic was simulated using a surface-complexation model (Dzombak and Morel, 1990; Parkhurst and Appelo, 1999). This approach allows the simulation of arsenic adsorption in complex natural environments (Grossl and Sparks, 1995). Laboratory experiments and field studies (Jain and Loeppert, 2000; Swedlund and Webster, 1999) demonstrate that arsenic adsorption by iron oxide is affected by other anions, including phosphate and silica, at concentrations found in many ground-water systems. Competitive adsorption between arsenic and other anions for the same adsorption sites on a solid also was simulated using the surface-complexation model in PHREEQC. Competitive adsorption is more complex than is represented by the surface-complexation model of Dzombak and Morel (1990). Recent laboratory investigation into the adsorption of As(V) and phosphate on goethite (α-FeOOH) produced results that are incompatible with a surface-complexation model (Hongshao and Stanforth, 2001). Of particular importance is the observation that goethite contains a non-exchangeable fraction for As(V) and phosphate, which means that sequential addition of the adsorbents results in a different aqueous composition than is obtained when the adsorbents are introduced concurrently. Consequently, the mathematical approach used in the simulations may result in higher aqueous arsenic concentrations being predicted than would be expected on the basis of the laboratory studies (see Hongshao and Stanforth, 2001; Manning and Goldberg, 1996).

Data used to simulate the water quality during recharge include temperature, chemistry of the recharge water, mineralogy and chemistry of the aquifer materials, and aquifer porosity. The chemical information on the aquifer material is limited to analyses of a few samples.

If all the oxygen in the recharge is consumed by oxidation of DOC, then iron and manganese oxides can dissolve. The reaction of dissolved oxygen with organic carbon commonly is written as:

$$CH_2O + O_2 \rightarrow CO_2 + H_2O \qquad (2)$$

The stoichiometry of this reaction indicates that ground water with 8 mg/L of dissolved oxygen can oxidize about 3 mg/L of organic carbon. Although not all of the DOC will necessarily react with oxygen, the amount of DOC in some samples collected from the S-Line Canal is large enough (Appendix 1) that it could consume all of the dissolved oxygen and then react with iron and manganese oxides. The reaction of DOC with these oxides could produce undesirable concentrations of iron and manganese in addition to releasing other trace inorganic constituents that commonly are contained within and on the surface of these oxides. The simulations assume that the recharge contains enough dissolved oxygen that iron and manganese oxides will not dissolve. Most of the S-Line Canal water sampled has sufficient dissolved oxygen to oxidize all the particulate and dissolved organic carbon, which makes this assumption reasonable for most of the samples.

Changes in water chemistry resulting from an actual project to artificially recharge the basalt likely will differ to some degree from the results of simulations made here. Although the basalt is largely homogenous, the mineralogy and chemistry of the basalt at an actual project location may differ from what was used in the simulations. Similarly, the chemical composition of the S-Line Canal changes during the year and the chemical composition of water used during actual artificial recharge may be different from what was used in the simulations.

Table 5. Initial conditions and reactions used for geochemical modeling of injection and infiltration of surface water and its subsequent recovery.

Description of simulation	Influent water composition	Aquifer material composition	Reactions
		Well injection	
W1. Equilibrate aquifer material with native ground water to set initial conditions.	Native ground water from site B-3 (sampled 06-30-99; Appendix 1).	Total number of cation exchange sites and iron-oxide surface from extraction of basalt core samples DB-1 442A and B.	Equilibrate native ground water with the aquifer material in reaction cells.
W2. Injection of surface water.	S-Line Canal water (sampled 05-14-01; Appendix 1).	Composition produced in simulation W1.	Inject surface water into reaction cells. Equilibrate with calcite, cation exchange, and iron oxide (closed with respect to CO_2).
W3. Withdrawal of injected water.	Native ground water from site B-3 (sampled 6-30-99; Appendix 1).	Composition produced in simulation W1.	Withdraw injected water from reaction cells and replace with native ground water. Equilibrate with calcite, cation exchange, and iron oxide (closed with respect to CO_2).
		Basin infiltration	
B1. Cell one, equilibrate recharge with cinder.	S-Line Canal water (sampled 05-14-01; Appendix 1).	Total number of cation exchange sites and iron-oxide surface from extraction of cinder outcrop samples RSHCA and RSHCB (table 2D).	Equilibration with atmospheric CO_2 (pCO_2 = -3.5 atmospheres) to simulate exposure to the atmosphere. React water with cinder.
B2. Cell two, equilibrate with water reacted with basalt cinder.	Water from previous reaction in cell one.	Cation exchange sites and iron-oxide surface from extraction results of vesicular outcrop sample RSHO (table 2D).	Equilibrate water from cell one with vesicular outcrop. Equilibration with atmospheric CO_2 (pCO_2 = -3.5 atmospheres) to simulate exposure to the atmosphere.
B3. Cells three through ten, initial aquifer and recharge composition.	Ground water from site B-3 (sampled 06-30-99; Appendix 1).	Total number of cation exchange sites and iron-oxide surface from extraction of basalt core samples DB-1 442A and B.	Equilibrate water with the basalt composition in reaction cells.
B4. Cells three through ten, infiltration into the basalt aquifer.	Composition after reaction in cell two.	Total number of cation exchange sites and iron-oxide surface from extraction of basalt core samples DB-1 442A and B.	Inject surface water into reaction cells. Equilibrate with calcite, cation exchange and iron oxide (closed with respect to CO_2).
B5. Cells three through ten, withdrawal.	Ground water from site B-3 (sampled 06-30-99; Appendix 1).	Composition produced in B3.	Withdraw injected water with inflow of B-3 water into reaction cells three through ten. Equilibration with calcite, cation exchange and iron oxide (closed with respect to CO_2).

Another way actual results may differ from simulated results is that the modeling approach assumes that lateral flow does not affect the ground-water quality of recovered water. Lateral flow would move the injected/infiltrated water away from the recharge site, replacing it with native ground water. This would decrease the removal of arsenic because of re-equilibration of arsenic in the ground water with the exchange sites. Factors which increase the amount of lateral flow, such as higher lateral-flow rates and longer times between recharge and withdrawal can lead to less efficient removal of arsenic.

Model Results

The chemical modeling involved reaction cells to simulate water chemistry during recharge and withdrawal. During the recharge phase in the well-injection model, surface water is injected into the first cell, displacing the native ground water from cell one to cell two. Following equilibration with the aquifer material, additional surface water is injected into cell one, displacing the now modified surface water from cell one to cell two. This sequence was repeated for 10 reaction steps until all 10 cells contained injected surface water. During the withdrawal phase, the process is reversed and water is removed from cell one and sequentially replaced by water from cells two through ten. Withdrawal continues until native ground water has replaced injected surface water in the 10 cells.

The results shown in figure 13 are the simulations for the first cell of the well-injection model, with the first cell representing a single well that both injects and withdraws water. Simulated pH, and arsenic and chloride concentrations during a single cycle of injection and withdrawal are shown in figure 13A and following multiple cycles are shown in figure 13B.

Modeling injection of water with a chemical composition similar to that of the S-Line Canal into the basalt aquifer and then withdrawing the water suggests that arsenic concentrations in the withdrawn water will be higher than in the injected water (fig. 13A). The results in cell one shown on figure 13A represent the composition of the water that moves into the next cell as outlined in table 5. The results for cell one represent the composition of the recovered water during the withdrawal cycle. The injection and withdrawal can be discussed in terms of three periods. During the first period, as water is being injected into the aquifer, chloride concentrations drop and pH increases to nearly 10 during the first reaction step. During reaction steps 2–10, arsenic concentrations jump as arsenic desorbs from the basalt and then decreases as the arsenic is transported out of the reaction cells. During the second period, as the injected water is withdrawn for the following 10 reaction steps, arsenic concentrations increase as injected water that had moved away from the well head now returns. In the third period, starting at reaction step 20, chloride concentrations jump sharply, indicating the return of native basalt-aquifer water. The pH in the withdrawn water returns to that normally found in the basalt aquifer after a few reaction steps during this last period. The lower pH causes an abrupt arsenic decrease, followed by a gradual increase to a value close to that normally found in the basalt aquifer over the next 30 reaction steps.

A second model consisted of simulating a series of injection and withdrawal cycles. An important difference between this model and that described above is that more water is injected than withdrawn, with withdrawal being limited to retrieval to the point where native basalt-aquifer water reaches cell two, but not cell one. Accordingly, the chloride concentrations in cell one always remain equal to the concentration in the injected water (fig. 13B). The pH and arsenic values during the first injection-withdrawal cycle are the same as described for the first two periods described above. During subsequent injection-withdrawal cycles, the arsenic and pH values show the same patterns with a progressive decrease with each succeeding cycle. The decreasing pH, which causes the lower arsenic concentrations, is a result of progressively less calcite dissolution. The decreasing calcite dissolution is a result of reduced exchange of calcium for sodium, which promotes calcite dissolution, as shown by reaction (1).

The basin-infiltration model differs from the well-injection model in that it includes two additional cells that represent the cinder and vesicular basalt in the unsaturated zone above the water table. The third cell represents the saturated zone below the infiltration basin. Results for this third cell are shown in figure 14 and describe the water quality at a withdrawal well tapping ground water below the basin. Simulations of water infiltrating through the unsaturated zone indicate potential for high arsenic concentrations in withdrawn ground water (fig. 14). Two scenarios are represented in figure 14 and differ in the amount of arsenic present in the iron oxide in the unsaturated zone. The first model represents iron oxide with no initial arsenic (fig. 14A). The second model assumes the iron oxide has equilibrated with a water composition like that of the infiltrating water except containing 10 µg/L of arsenic (fig. 14B). The results show similar patterns, although the arsenic concentrations in the recovered water are higher for the model represented in figure 14B because of the greater amount of arsenic in the unsaturated zone, particularly during the first scenario.

Because the amount of carbon dioxide in the unsaturated zone affects carbonate solubility, it also could affect arsenic concentrations. The simulation results shown in figures 13–14 used atmospheric concentrations of carbon dioxide (pCO_2 of $10^{-3.5}$). However, similar arsenic and pH results were obtained using a higher pCO_2 of $10^{-2.5}$, which is similar to observed pressures in the soil zone (data not shown).

The model results indicate the potential for unacceptably high arsenic concentrations in recovered ground water; however, simulated arsenic concentrations in the recovered water may overestimate concentrations during real recharge operations. First, the models do not consider the effect of

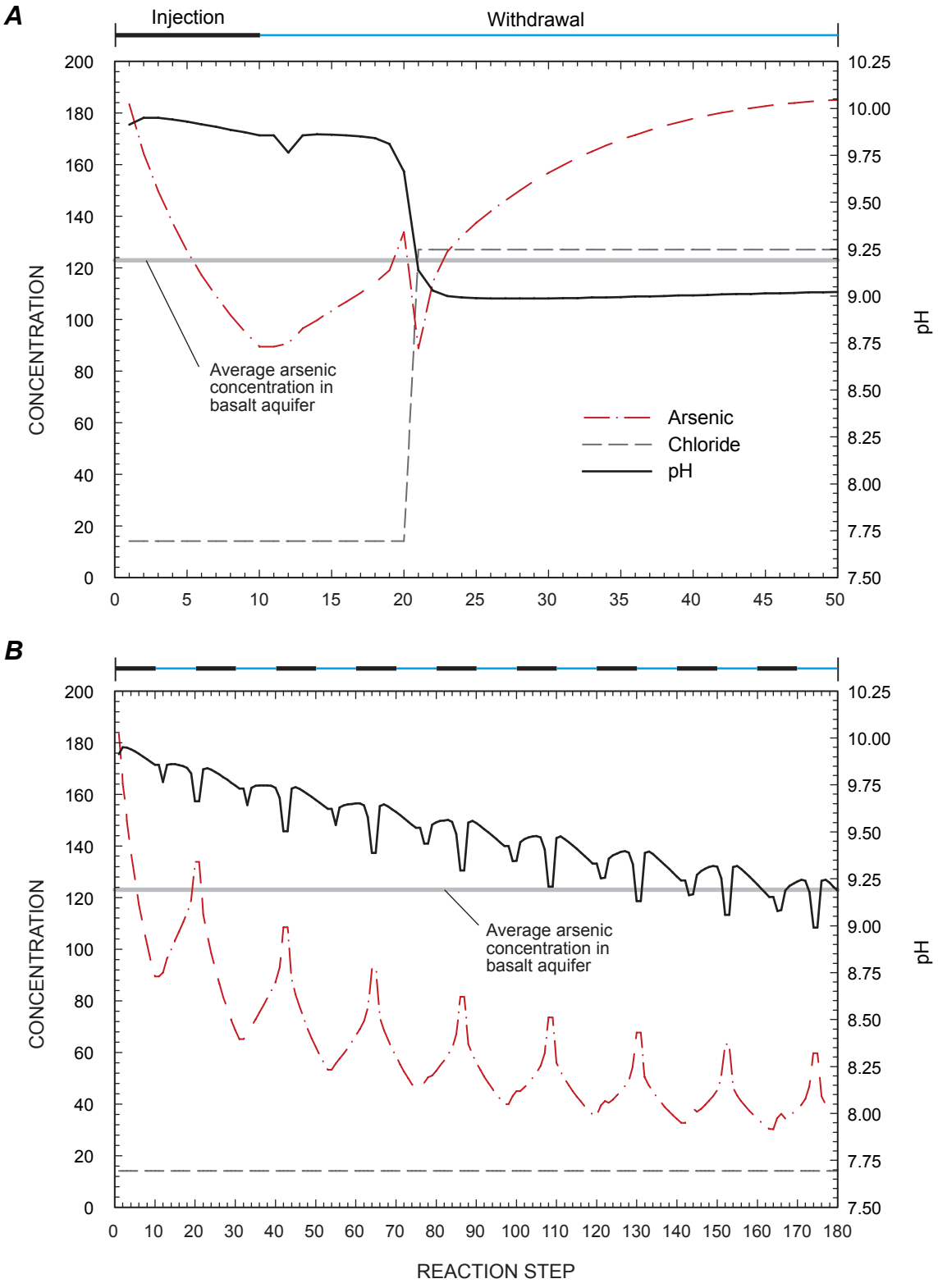

Figure 13. Results of geochemical simulation of injection well model of recharge into the basalt aquifer. Model scenarios are for a (***A***) single cycle and (***B***) multiple cycles. Concentration units are µg/L for arsenic and mg/L for chloride. Black and blue horizontal lines at top of graphs represent injection and withdrawal cycles.

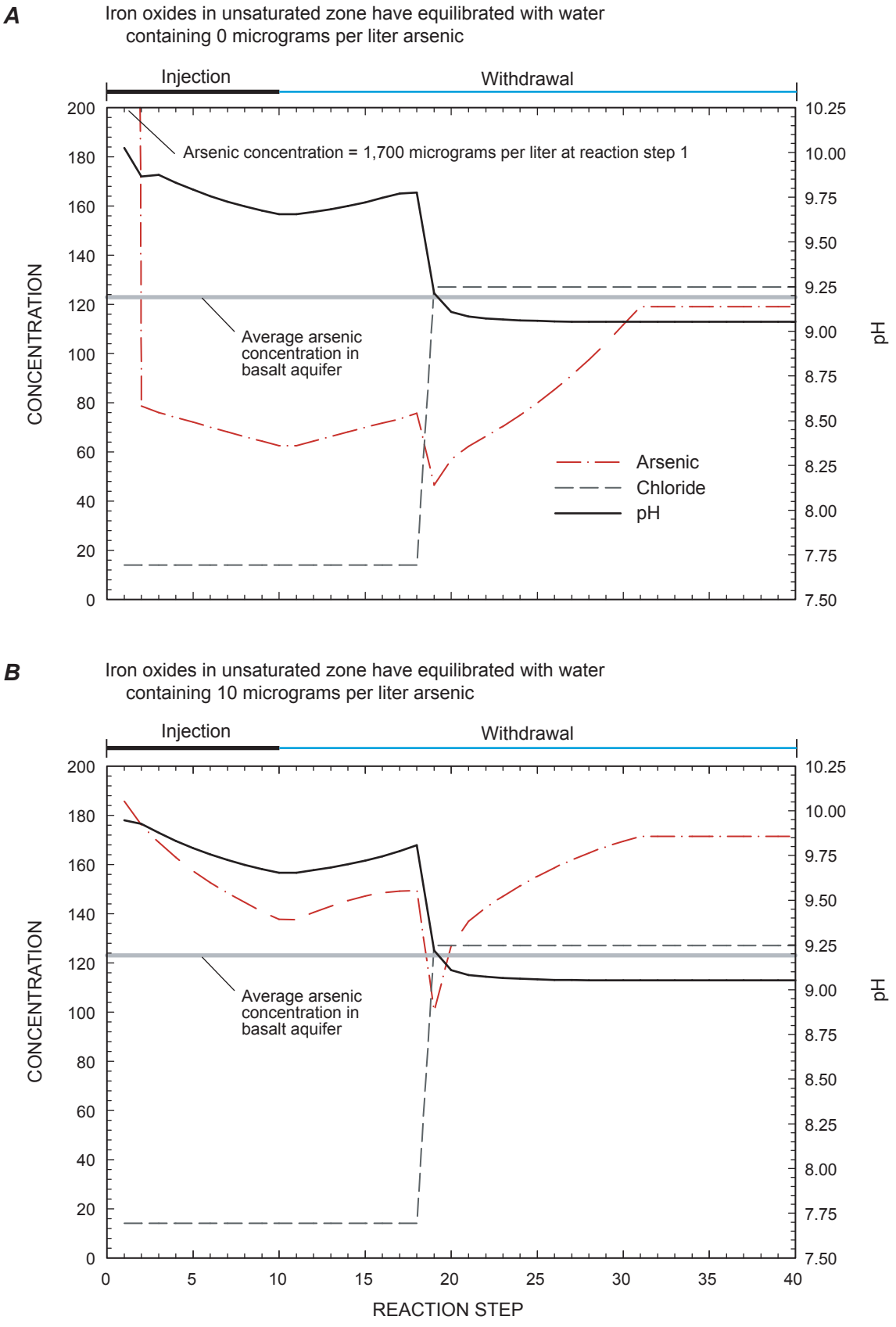

Figure 14. Results of geochemical simulation of basin-infiltration model of recharge into the basalt aquifer. Model scenarios are for iron oxide equilibrated with water containing (***A***) no arsenic and (***B)*** 10 µg/L arsenic. Concentration units are µg/L for arsenic and mg/L for chloride. Black and blue horizontal lines at top of graphs represent injection and withdrawal cycles, respectively.

lateral flow of ground water between injection and recovery. Second, released arsenic may be less because the model uses adsorption parameters for HFO that may overestimate the amount of arsenic released to ground water. The retention of arsenic in iron oxide is an important factor when considering a long-term recharge effort. The transformation of freshly precipitated iron oxide into a more crystalline form needs to be considered. Field (Mettler, 2002) and laboratory (Ford, 2002) studies suggest that this process may occur at a rate that can be important for long-term recharge projects. Laboratory aging of HFO coprecipitated with As(V) shows a half-life for transformation into goethite of about 300 days at 25°C in the presence of dissolved oxygen (Ford, 2002). The transformation was not accompanied by a release of arsenic into solution. The applicability of these laboratory experiments to field settings has not been well studied.

The effects of flushing of constituents such as chloride and sulfate that may be present in the unsaturated zone beneath Rattlesnake Hill were not considered in the basin-infiltration model. These and other soluble salts may have been added to the basalt exposed at Rattlesnake Hill during the dessication of Lake Lahontan and subsequently by rainfall and dust. Flushing of these solutes may be important during the early phase of a recharge effort and could decrease as they are leached out of the unsaturated zone.

Summary and Conclusions

The Fallon basalt aquifer serves as the sole source of municipal water for Lahontan Valley in west-central Nevada. The principal users include the City of Fallon, Naval Air Station Fallon, and the Fallon Paiute-Shoshone Tribe. Increased pumpage from the aquifer has been accompanied by declines in water levels and changes in water quality. Storage of surface water in the basalt may mitigate the effects of increased pumpage, but may cause undesirable changes in water chemistry. Water-quality samples of the S-Line Canal, a likely source of water for augmentation of recharge, indicates that with the exception of arsenic, the water is acceptable for water supply. Because the arsenic in ground water of the basalt aquifer exceeds drinking water standards, the potential for arsenic release to artificial recharge was explored by using geochemical modeling. Model results inidcate that arsenic release from the basalt may increase its concentrations in ground water to levels that could limit the use of artificial recharge. Model results for well injection indicate that arsenic concentrations may initially increase following artificial recharge, but decline with repeated cycles of injection and withdrawal. Field based experiments are needed to evaluate the underlying model assumptions.

Arsenic concentrations in withdrawn water following artificial recharge could be limited by increasing adsorption onto the basalt aquifer. Field and laboratory experiments show that a combination of increasing the iron oxide content of the basalt aquifer and lowering the pH of the ground water could decrease arsenic concentrations (Welch and others, 2003). The short- and long-term effects of artificial recharge on arsenic concentrations could be evaluated through similar experimental approaches described by these authors.

Surface infiltration has several advantages over well injection and the high permeability of scoriaceous cinders near the top of Rattlesnake Hill could make this a good location from the standpoint of allowing rapid infiltration. Clay and larger size particles in recharge water that often reduce the infiltration and injection rates can be mechanically removed from the surface of an infiltration basin. In contrast, rehabilitating a well clogged by the clay particles in recharge water may be very expensive or impossible. Nonetheless, the cinders have a large reactive surface area that could lead to undesirable geochemical reactions. In such a case, surface infiltration may not be a desirable approach. Additional field-based experiments are needed to evaluate which approach is the best.

References Cited

Appelo, C.A.J., Van Der Weiden, M.J.J., Tournassat, C., and Charlet, L., 2002, Surface complexation of ferrous iron and carbonate on ferrihydrite and the mobilization of arsenic: Environmental Science & Technology, v. 36, p. 3096–3103.

Axelrod, D.I., 1956, Mid-Pliocene floras from west-central Nevada: University of California—Publications in Geological Sciences, v. 33, p. 322.

Benson, L.V., 1991, Timing of the last high stand of Lake Lahontan: Journal of Paleolimnology, v. 5, p. 115–126.

Benson, L.V., Currey, D.R., Dorn, R.I., Lajoie, K.R., Oviatt, C.G., Robinson, S.W., Smith, G.I., and Stine, S., 1990, Chronology of expansion and contraction of four Great Basin lake systems during the past 35,000 years: Paleogeography, Paleoclimatology, and Paleoecology, v. 78, p. 241–286.

Berris, S.N., Crompton, E.J., Joyner, J.D., and Ryan, Rosalyn, 2003, Water resources data—Nevada, Water Year 2002: U.S. Geological Survey Water-Data Report NV-02-1, 600 p.

Bureau of Reclamation, 1987, Final environmental impact statement for the Newlands Project proposed operating criteria and procedures: Washington D.C., p. 332.

Capel, P.D., and Larson, S.J., 1996, Evaluation of selected information on splitting devices for water samples: U.S. Geological Survey Water-Resources Investigations Report 95–4141, 103 p.

Coplen, T.B., Wildman, J.D., and Chen, J., 1991, Improvements in the gaseous hydrogen-water equilibration technique for hydrogen isotope ratio analysis: Analytical Chemistry, v. 63, no. 9, p. 910–912.

Davis, J.O., 1978, Quaternary tephrochronology of the Lake Lahontan area, Nevada and California: University of Nevada, Reno, Nevada Archeological Survey Research Paper 7, 137 p.

Dzombak, D.A., and Morel, F.M.M., 1990, Surface complexation modeling: Hydrous Ferric Oxide, New York, Wiley, 393 p.

Epstein, S., and Meyeda, T., 1953, Variation of O-18 content of water from natural sources: Geochimica at Cosmochimica Acta, v. 4, p. 213–224.

Evans, S.H.J., 1980, Summary of potassium/argon age dating—1979: University of Utah, Department of Geology and Geophysics Topical Report, 23 p.

Federal Register, 2001, National primary drinking water regulations: Arsenic and clarifications to compliance and new source contaminants monitoring—Final rule: Office of the Federal Register, v. 66, no. 14, p. 6975–7066.

Fishman, M.J., ed., 1993, Methods of analysis by the U.S. Geological Survey National Water Quality Laboratory—Determination of inorganic and organic constituents in water and fluvial sediments: U.S. Geological Survey Open-File Report 93–125, 217 p.

Fishman, M.J., and Friedman, L.C., 1989, Methods for the determination of inorganic substances in water and fluvial sediments: U.S. Geological Survey Techniques of Water-Resources Investigations, Book 5, Chapter A1, 545 p.

Ford, R.G., 2002, Rates of hydrous ferric oxide crystallization and the influence on coprecipitated arsenate: Environmental Science & Technology, v. 36, p. 2459–2463.

Garbarino, J.R., 1999, Methods of analysis by the U.S. Geological Survey National Water Quality Laboratory—Determination of dissolved arsenic, boron, lithium, selenium, strontium, thallium, and vanadium using inductively coupled plasma-mass spectrometry: U.S. Geological Survey Open-File Report 99–093, 31 p.

Glancy, P.A., 1986, Geohydrology of the basalt and unconsolidated sedimentary aquifers in the Fallon area, Churchill County, Nevada: U.S. Geological Survey Water-Supply Paper 2263, 62 p.

Grossl, P.R., and Sparks, D.L., 1995, Evaluation of contaminant ion adsorption/desorption on goethite using pressure-jump relaxation kinetics: Geoderma, v. 67, p. 87–101.

Hongshao, Z., and Stanforth, R., 2001, Competitive adsorption of phosphate and arsenate on goethite: Environmental Science & Technology, v. 35, p. 4753–4757.

Jain, A., and Loeppert, R.H., 2000, Effect of competing anions on the adsorption of arsenate and arsenite by ferrihydrite: Journal of Environmental Quality, v. 29, p. 1422–1430.

Jones, S.R., and Garbarino, J.R., 1999, Methods of analysis by the U.S. Geological Survey National Water Quality Laboratory—Determination of arsenic and selenium in water and sediment by graphite furnace-atomic absorption spectrometry: U.S. Geological Survey Open-File Report 98–639, 39 p.

Le Maitre, R.W., 1976, The chemical variability of some common igneous rocks: Journal of Petrology, v. 17, p. 589–637.

Lico, M.S., and Seiler, R.L., 1994, Ground-water quality and geochemistry, Carson Desert, western Nevada: U.S. Geological Survey Open-File Report 94–31, 91 p.

Madsen, J.E., Sandstrom, M.W., and Zaugg, S.D., 2003, Methods of analysis by the U.S. Geological Survey National Water Quality Laboratory—A method supplement for the determination of Fipronil and degradates in water by gas chromatography/mass spectrometry: U.S. Geological Survey Open-File Report 02–462, 11 p.

Manning, B.A., and Goldberg, S., 1996, Modeling arsenate competitive adsorption on kaolinite, montmorillonite and illite: Clays and Clay Minerals, v. 44, p. 609–623.

Maurer, D.K., 2002, Results of test drilling in the basalt aquifer near Fallon, Nevada: U.S. Geological Survey Fact Sheet, FS–048–02, 4 p.

Maurer, D.K., and Welch, A.H., 1996, Hydrogeology and potential effects of changes in water use, Carson Desert agricultural area, Churchill County, Nevada: U.S. Geological Survey Water Supply Paper 2436, 106 p.

Maurer, D.K., and Welch, A.H., 2001, Hydrogeology and geochemistry of the Fallon basalt and adjacent aquifers in Churchill County, Nevada, and potential sources of basalt recharge: U.S. Geological Survey Water-Resources Investigations Report 01–4130, 72 p.

Mettler, S., 2002, In situ iron removal from ground water—Fe(II) oxygenation, and precipitation products in a calcareous aquifer: Zurich, Swiss Federal Institute of Technology, Ph.D. Dissertation, 146 p.

Morrison, R.B., 1964, Lake Lahontan—Geology of southern Carson Desert, Nevada: U.S.: Geological Survey Professional Paper 401, 156 p.

Morrison, R.B., 1991, Quaternary stratigraphic, hydrologic, and climatic history of the Great Basin, with emphasis on Lakes Lahontan, Bonneville, and Tecopa, *in* Morrison, R.B., ed., The Geology of North America, Quaternary Nonglacial Geology—Conterminous U.S. Geological Society of America, p. 283–320.

Owenby, J.R., and Ezell, D.S., 1992, Monthly station normals of temperature, precipitation, and heating and cooling degree days, 1961–1990, Nevada: National Climatic Data Center Report 81, 20 p.

Parkhurst, D.L., and Appelo, C.A.J., 1999, User's guide to PHREEQC (version 2): U.S. Geological Survey Water-Resources Investigations Report 99–4259, 312 p.

Patton, C.J., and Truitt, E.P., 2000, Methods of analysis by the U.S. Geological Survey National Water Quality Laboratory—Determination of ammonium plus organic nitrogen by a Kjeldahl digestion method and an automated photometric finish that includes digest cleanup by gas diffusion: U.S. Geological Survey Open-File Report 00–170, 31 p.

Redman, A.D., Macalady, D.L., and Ahmann, D., 2002, Natural organic matter affects arsenic speciation and sorption onto hematite: Environmental Science & Technology, v. 36, p. 2889–2896.

Stollenwerk, K.G., 2003, Geochemical processes controlling transport of arsenic in groundwater—A review of adsorption, *in* Welch, A.H., and Stollenwerk, K.G., eds., Arsenic in ground water: Geochemistry and Occurrence, Boston, Mass., Kluwer Academic Publishers, p. 67–100.

Struzeski, T.M., DeGiacomo, W.J., and Zayhowski, E.J., 1996, Methods of analysis by the U.S. Geological Survey National Water Quality Laboratory—Determination of dissolved aluminum and boron in water by inductively coupled plasma-atomic emission spectrometry: U.S. Geological Survey Open-File Report 96–149, 17 p.

Sumner, M.E., and Miller, W.P., 1996, Cation exchange capacity and exchange coefficients, methods of soil analysis—Part 3. chemical methods: Soil Science Society of America, p. 1218–1220.

Swedlund, P.J., and Webster, J.G., 1999, Adsorption and polymerisation of silicic acid on ferrihydrite, and its effect on arsenic adsorption: Water Research, v. 33, p. 3413–3422.

Tessier, A., Campbell, P.G.C., and Bisson, M., 1979, Sequential extraction procedure for the speciation of particulate trace metals: Analytical Chemistry, v. 51, p. 844–851.

Thatcher, L.L., Janzer, V.J., and Edwards, K.W., 1977, Methods for determination of radioactive substances in water and fluvial sediments: U.S. Geological Survey Techniques of Water-Resources Investigations, Book 5, Chapter A5, 95 p.

Van Geen, A., Robertson, A.P., and Leckie, J.O., 1994, Complexation of carbonate species at the goethite surface—implications for adsorption of metal ions in natural waters: Geochimica et Cosmochimica Acta, v. 58, p. 2073–2086.

Welch, A.H., and Lico, M.S., 1998, Factors controlling As and U in shallow ground water, southern Carson Desert, Nevada: Applied Geochemistry, v. 13, no. 4, p. 521–539.

Welch, A.H., Stollenwerk, K.G., Maurer, D.K., and Feinson, L.S., 2003, In situ arsenic remediation in a fractured, alkaline aquifer, *in* Welch, A.H., and Stollenwerk, K.G., eds., Arsenic in Ground Water, Geochemistry and Occurrence: Boston, Mass., Kluwer Academic Publishers, p. 403–419.

Welch, A.H., Westjohn, D.B., Helsel, D.R., and Wanty, R.B., 2000, Arsenic in ground water of the United States—Occurrence and geochemistry: Ground Water, v. 38, no. 4, p. 589–604.

Wilde, F.D., and Radtke, D.B., eds., 1998, National Field Manual for the collection of water-quality data: U.S. Geological Survey Techniques of Water-Resources Investigations, Book 9, Chapter A6, 128 p.

Zaugg, S.D., Sandstrom, M.W., Smith, S.G., and Fehlberg, K.M., 1995, Methods of analysis by the U.S. Geological Survey National Water Quality Laboratory—Determination of pesticides in water by C-18 solid-phase extraction and capillary-column gas chromatography/mass spectrometry with selected-ion monitoring: U.S. Geological Survey Water-Resources Investigations Report 95–181, 49 p.

Zaugg, S.D., Smith, S.G., Schroeder, M.P., Barber, L.B., and Burkhardt, M.R., 2002, Methods of analysis by the U.S. Geological Survey National Water Quality Laboratory—Determination of wastewater compounds by polystyrene-divinylbenzene solid-phase extraction and capillary-column gas chromatography/mass spectrometry: U.S. Geological Survey Water-Resources Investigations Report 01–4186, 37 p.

APPENDIXES

Appendix 1. Field measurements and concentrations of major ions, nutrients, trace elements, radionuclides, and organic carbon in water samples from S-Line Canal at Cemetery Bridge and USGS basalt well B-3 collected from October 1997 to October 2002.

[Abbreviations and symbols: ºC, degrees Celsius; E, estimated concentration; ft^3/s, cubic feet per second; ft, feet; mm, millimeters; M, presence verified but not quantified; mg/L, milligrams per liter; nm, nanometer; pCi/L, picoCuries per liter; UV, ultraviolet; µS/cm, microsiemens per centimeter at 25 ºC; µg/L, microgram per liter; <, less than; --, not determined or not applicable. All concentrations were determined on filtered samples unless otherwise noted.]

Site (fig. 3)	U.S. Geological Survey Site identifier	Date	Time	Well depth	Daily mean stream discharge (ft^3/s)	pH (units)	Air temperature (ºC)	Water temperature (ºC)	Dissolved oxygen (mg/L)	Specific conductance (uS/cm)	UV absorbance at 254 nm	UV absorbance at 280 nm
Surface Water												
S-Line Canal	1031220115	05-14-01	1120	--	23	8.5	27.5	15.6	7.8	275	--	--
		06-19-01	1045	--	16	8.5	28.5	19.8	8.0	288	--	--
		07-25-01	1050	--	.06		31	21.2	7.6	290	--	--
		08-21-01	925	--	.05	7.6	28.5	19.8	8.2	301	--	--
		10-17-01	1015	--	18	9.1	20.5	14.4	8.0	320	--	--
		04-08-02	1015	--	.38	9.0	18.5	12.6	8.2	371	--	--
		06-25-02	1015	--	.11	7.7	--	19.0	7.9	283	--	--
		08-27-02	1045	--	28	7.4	--	19.8	7.9	293	--	--
		10-18-02	1115	--	17	9.4	--	13.8	7.7	297	0.065	0.046
Ground Water												
Well B-3	392914118442701	10-20-97	1500	71	--	9.1	--	22.5	.9	1,110	--	--
		06-30-99	1000	71	--	9.3	--	22	.4	1,120	--	--

Appendix 1. Field measurements and concentrations of major ions, nutrients, trace elements, radionuclides, and organic carbon in water samples from S-Line Canal at Cemetery Bridge and USGS basalt well B-3 collected from October 1997 to October 2002—Continued

Site (fig. 3)	Date	Calcium (mg/L as Ca)	Magnesium (mg/L as Mg)	Sodium (mg/L as Na)	Potassium (mg/L as K)	Bicarbonate (mg/L as HCO_3)	Carbonate (mg/L as CO_3)	Alkalinity (mg/L as $CaCO_3$)	Sulfate (mg/L as SO_4)	Chloride (mg/L as Cl)	Bromide (mg/L as Br)	Fluoride (mg/L as F)	Iodide (mg/L as I)	Silica (mg/L as Si)	Total dissolved solids (mg/L)
						Surface Water									
S-Line Canal	05-14-01	21.1	5.86	25.8	3.39	98	0	81	29.6	14.0	--	.2	--	18.8	171
	06-19-01	23.6	6.46	26.4	3.48	99	0	81	36.5	14.1	--	.3	--	19.5	198
	07-25-01	22.2	6.12	27.4	3.61	99	0	81	36.0	13.3	--	.2	--	19.7	189
	08-21-01	24.0	6.53	26.7	3.62	109	0	90	38.0	13.6	--	.2	--	20.5	194
	10-17-01	23.1	6.57	28.3	3.72	111	0	91	43.1	16.1	--	.3	--	19.1	210
	04-08-02	27.4	7.83	38.0	4.05	126	0	104	48.4	21.7	--	.3	--	18.1	230
	06-25-02	22.2	6.34	26.4	3.23	95	0	78	35.3	15.4	--	.15	--	19.2	185
	08-27-02	22.7	6.25	26.3	3.42	101	0	83	36.3	12.3	--	.25	--	20.4	193
	10-18-02	22.3	6.44	28.7	3.65	97	0	80	36.8	13.8	--	.22	--	20.4	199
						Ground Water									
Well B-3	10-20-97	1.72	.904	236	7.8	245	30	251	102	130	.21	.8	.004	24.6	672
	06-30-99	1.67	.651	232	7.92	250	45	280	100	127	.22	.9	--	24.7	--

Appendix 1. Field measurements and concentrations of major ions, nutrients, trace elements, radionuclides, and organic carbon in water samples from S-Line Canal at Cemetery Bridge and USGS basalt well B-3 collected from October 1997 to October 2002—Continued

Site (fig. 3)	Date	Nitrate plus nitrite (mg/L as N)	Nitrite (mg/L as N)	Ammonia (mg/L as N)	Ammonia plus organic nitrogen (mg/L as N)	Ammonia plus organic nitrogen, total (mg/L as N)	Nitrogen, particulate (mg/L as N)	Total phosphorus whole water (mg/L as P)	Total phosphorus filtered (mg/L as P)	Ortho-phosphate filtered (mg/L as P)	Carbon, inorganic plus organic, total (mg/L as C)	Carbon, inorganic plus organic, particulate (mg/L as C)
						Surface Water						
S-Line Canal	05-14-01	0.17	0.015	0.05	0.27	0.45	0.09	0.131	0.073	0.06	0.7	M
	06-19-01	.15	.007	<.04	.20	.40	.16	.131	.079	.07	1.3	<.1
	07-25-01	.14	E.003	<.04	.20	.39	.32	.190	.094	.08	2.0	<.1
	08-21-01	.12	<.006	<.04	.22	.43	.16	.164	.109	.09	1.3	<.1
	10-17-01	.09	<.008	<.04	.21	.39	.19	.196	.113	.09	1.4	<.1
	04-08-02	<.05	<.008	<.04	.21	.34	.12	.105	.081	.05	0.6	
	06-25-02	E.03	<.008	<.04	.14	.34	.18	.139	.085	.07	1.2	<.1
	08-27-02	.05	<.008	<.04	.19	.31	.11	.141	.097	.09	0.7	<.1
	10-18-02	<.06	<.008	<.04	.19	.33	.10	.162	.111	.08	0.7	<.1
						Ground Water						
Well B-3	10-20-97	--	--	--	--	--	--	--	--	.27	--	--
	06-30-99	--	--	--	--	--	--	--	--	--	--	--

Appendix 1. Field measurements and concentrations of major ions, nutrients, trace elements, radionuclides, and organic carbon in water samples from S-Line Canal at Cemetery Bridge and USGS basalt well B-3 collected from October 1997 to October 2002—Continued

Site (fig. 3)	Date	Carbon, organic, dissolved (mg/L as C)	Carbon, organic, particulate (mg/L as C)	Alum-inum (µg/L As Al)	Antimony (µg/L as Sb)	Arsenic (µg/L as As)	Barium (µg/L as Ba)	Beryllium (µg/L as Be)	Boron (µg/L as B)	Cadmium (µg/L as Cd)	Chro-mium (µg/L as Cr)	Cobalt (µg/L as Co)	Copper (µg/L) as Cu	Iron (µg/L as Fe)	Lead (µg/L as Pb)	Lithium (µg/L as Li)
Surface Water																
S-Line Canal	05-14-01	2.9	E.7	1	0.10	1.5	82	<.06	44	<.04	<.8	0.27	1.1	<10	<0.08	4.2
	06-19-01	2.5	1.3	2	.48	10.9	33	<.06	246	0.04	<.8	.11	2.1	<10	.13	27.1
	07-25-01	5.8	2.0	2	.52	10.0	33	<.06	259	E.03	<.8	.12	1.9	<10	<.08	30.7
	08-21-01	3.7	1.2	1	.48	10.8	34	<.06	233	E.02	<.8	.10	2.5	<10	<.08	25.4
	10-17-01	--	1.4	1	.47	10.4	33	<.06	259	<.04	<.8	.12	2.7	<10	<.08	28.5
	04-08-02	--		1	.35	13.7	38	<.06	380	E.04	<.8	.16	2.2	<10	.13	40.6
	06-25-02	--	1.2	2	.49	10.2	34	<.06	242	E.03	<.8	.12	2.5	<10	<.08	28.5
	08-27-02	4.0	.7	2	.51	11.2	33	<.06	215	E.03	<.8	.10	2.9	<10	<.08	24.5
	10-18-02	5.4	.7	<2	.56	11.2	31	<.06	253	E.02	<.8	.11	2.4	<10	.16	24.9
Ground Water																
Well B-3	10-20-97	0.7	--	--	--	135	--	--	--	--	--	--	--	5	--	--
	06-30-99	--	--	--	--	123	--	--	--	--	--	--	--	<10	--	--

Appendix 1. Field measurements and concentrations of major ions, nutrients, trace elements, radionuclides, and organic carbon in water samples from S-Line Canal at Cemetery Bridge and USGS basalt well B-3 collected from October 1997 to October 2002—Continued

Site (fig. 3)	Date	Manganese (µg/L as Mn)	Mercury (µg/L as Hg)	Mercury, Total (µg/L as Hg)	Molybdenum (µg/L as Mo)	Nickel (µg/L as Ni)	Selenium (µg/L as Se)	Silver (µg/L as Ag)	Strontium (µg/L as Sr)	Thallium (µg/L as Tl)	Vanadium (µg/L as V)	Zinc (µg/L as Zn)
Surface Water												
S-Line Canal	05-14-01	5.5	--	0.24	1.5	0.5	0.4	<1	357	E0.04	3.6	2
	06-19-01	4.2	--	--	5.6	.29	<.3	<1	246	.07	6.6	<1
	07-25-01	3.9	--	.45	5.8	.29	<.3	<1	255	<.04	5.1	<1
	08-21-01	2.1	--	.34	6.3	<.06	E.2	<1	263	<.04	5.5	2
	10-17-01	1.9	--	.42	6.3	.65	E.3	<1	256	<.04	5.3	2
	04-08-02	9.4	0.01	.18	7.6	.61	<.3	<1	284	<.04	5.3	1
	06-25-02	7.5	--	.19	5.0	.36	E.2	<1	228	.16	5.2	1
	08-27-02	3.1	E.01	--	5.5	1.69	<.3	<1	242	<.04	5.7	1
	10-18-02	3.0	<.02	--	5.2	1.02	<.5	<.20	229	E.03	5.0	M
Ground Water												
Well B-3	10-20-97	<1.0	--	--	--	--	--	--	--	--	--	--
	06-30-99	<3.0	--	--	--	--	--	--	--	--	--	--

Appendix 1. Field measurements and concentrations of major ions, nutrients, trace elements, radionuclides, and organic carbon in water samples from S-Line Canal at Cemetery Bridge and USGS basalt well B-3 collected from October 1997 to October 2002—Continued

Site (fig. 3)	Date	Delta deuterium (per mil)	Delta oxygen-18 (per mil)	Alpha radioactivity (pCi/L as Th-230)	Alpha radioactivity, 2-sigma precision estimate (pCi/L as Th-230)	Gross beta radioactivity (pCi/L as Cs-137)	Beta radioactivity, 2-sigma precision estimate (pCi/L as Cs-137)	Radium-226 (pCi/L)	Radium-226, 2-sigma precision estimate (pCi/L)	Uranium, natural (μg/L)
					Surface Water					
S-Line Canal	05-14-01	-85.7	-10.35	<3	1.3	5	1.6	0.04	0.02	2.59
	06-19-01	-89.1	-10.48	3	1.4	6	1.7	.05	.02	3.88
	07-25-01	-88.2	-10.36	3	1.2	8	2.0	.06	.02	3.68
	08-21-01	-84.5	-9.92	3	1.1	6	1.8	.04	.02	3.76
	10-17-01	-81.0	-9.23	3	1.2	7	1.9	.05	.01	4.12
	04-08-02	-84.2	-10.00	5	1.8	9	2.2	.23	.05	5.62
	06-25-02	-90.1	-10.90	3	1.4	5	1.5	.03	.01	3.24
	08-27-02	-86.7	-10.32	2	1.2	7	2.0	.06	.02	3.42
	10-18-02	-86.5	-10.00	3	1.3	7	1.9	.04	.02	3.08
					Ground Water					
Well B-3	10-20-97	-110	-13.89	--	--	--	--	--	--	--
	06-30-99	--	--	--	--	--	--	--	--	--

Appendix 1. Field measurements and concentrations of major ions, nutrients, trace elements, radionuclides, and organic carbon in water samples from S-Line Canal at Cemetery Bridge and USGS basalt well B-3 collected from October 1997 to October 2002— Continued

Site (fig. 3)	Date	Carbon, inorganic plus organic, total (mg/L as C)	Carbon, inorganic plus organic, particulate (mg/L as C)	Carbon, organic, dissolved (mg/L as C)	Carbon, organic, particulate (mg/L as C)
			Surface Water		
S-Line Canal	05-14-01	0.7	M	2.9	E.7
	06-19-01	1.3	<.1	2.5	1.3
	07-25-01	2.0	<.1	5.8	2.0
	08-21-01	1.3	<.1	3.7	1.2
	10-17-01	1.4	<.1	--	1.4
	04-08-02	.6	--	--	--
	06-25-02	1.2	<.1	--	1.2
	08-27-02	.7	<.1	4.0	.7
	10-18-02	.7	<.1	5.4	.7
			Ground Water		
Well B-3	10-20-97	--	--	.7	--
	06-30-99	--	--	--	--

Appendix 2. Concentrations of organic compounds in water samples from S-Line Canal collected from Cemetery Bridge, May 2001 to October 2002

[All samples were filtered unless otherwise noted by "Total". Abbreviations and symbols: E, estimated value; M, presence verified, not quantified; --, not analyzed; <, less than]

Date	Time	1,4-Dichlorobenzene (µg/L)	1-Methylnaphthalene (µg/L)	2,6-Diethylaniline (µg/L)	2,6-Dimethylnaphthalene (µg/L)	2-Methylnaphthalene (µg/L)	3-Beta Coprostanol (µg/L)	3-Methyl-1(H)-indole (µg/L)	3-tert-butyl-4-hydroxyanisole (µg/L)	4-Cumylphenol (µg/L)	4-Octylphenol (µg/L)	4-tert-octylphenol (µg/L)	5-Methyl-1H-benzotriazole (µg/L)
05-14-01	1120	--	--	<0.002	--	--	--	--	--	--	--	--	--
06-19-01	1045	--	--	<.002	--	--	--	--	--	--	--	--	--
08-21-01	925	--	--	<.002	--	--	--	--	--	--	--	--	--
10-17-01	1015	<.5	<.5	<.002	<.5	<.5	<2	<1	<5	<1	<1	<1	<2
04-08-02	1015	<.5	<.5	<.006	<.5	<.5	<2	<1	<5	<1	<1	<1	<2
08-27-02	1045	<.5	<.5	<.006	<.5	<.5	M	<1	<5	<1	<1	<1	<2
10-18-02	1115	--	--	<.006	--	--	--	--	--	--	--	--	--

Date	Acetochlor (µg/L)	Acetophenone (µg/L)	Acetyl hexamethyltetrahydronaphthalene (µg/L)	Alachlor (µg/L)	Aldrin, Total (µg/L)	Alpha BHC (µg/L)	Anthracene (µg/L)	Anthraquinone (µg/L)	Atrazine (µg/L)	Benfluralin (µg/L)	Benzo(a)pyrene (µg/L)	Benzophenone (µg/L)	Betasitosterol (µg/L)	Bisphenol A (µg/L)	Bromacil (µg/L)
05-14-01	<.004	--	--	<.002	--	<.005	--	--	E.002	<.010	--	--	--	--	--
06-19-01	<.004	--	--	<.002	--	<.005	--	--	E.002	<.010	--	--	--	--	--
08-21-01	<.004	--	--	<.002	<.01	<.005	--	--	<.007	<.010	--	--	--	--	--
10-17-01	<.004	E.1	M	<.002	--	<.005	<.5	<.5	<.007	<.010	<.5	<.5	<2	3	<.5
04-08-02	<.006	<.5	<.5	<.004	--	<.005	<.5	<.5	<.007	<.010	<.5	<.5	<2	<1	E.2
08-27-02	<.006	E.1	<.5	<.004	<.01	<.005	<.5	<.5	<.007	<.010	<.5	<.5	<2	<1	<.5
10-18-02	<.006	--	--	<.007	--	<.005	--	--	<.007	<.010	--	--	--	--	--

Appendix 2. Concentrations of organic compounds in water samples from S-Line Canal collected from Cemetery Bridge, May 2001 to October 2002—Continued

Date	Bromoform (µg/L)	Butylate (µg/L)	Caffeine (µg/L)	Camphor (µg/L)	Carbaryl (µg/L)	Carbazole (µg/L)	Carbofuran (µg/L)	Chlordane, Total (µg/L)	Chlorpyrifos (µg/L)	Cholesterol (µg/L)	Cotinine (µg/L)	Cyanazine (µg/L)	DCPA (µg/L)	Deethylatrazine (µg/L)	Desulfinylfipronil (µg/L)
05-14-01	--	<.002	--	--	<.041	--	<.020	--	<.005	--	--	<.018	<.003	E.002	--
06-19-01	--	<.002	--	--	<.041	--	<.020	--	<.005	--	--	<.018	<.003	<.006	--
08-21-01	--	<.002	--	--	<.041	--	<.020	<.1	<.005	--	--	<.018	<.003	<.006	--
10-17-01	<.5	<.002	<.5	<.5	<1	<.5	<.020	--	<.5	M	<1	<.018	<.003	<.006	--
04-08-01	<.5	<.002	M	<.5	<.041	<.5	<.020	--	<.005	<2	<1	<.018	<.003	<.006	--
08-27-02	<.5	<.002	E.1	<.5	<.041	<.5	<.020	<.1	<.005	E1	<1	<.018	<.003	<.006	--
10-18-02	--	<.002	--	--	<.041	--	<.020	--	<.005	--	--	<.018	<.003	<.006	<.004

Date	Diazinon (µg/L)	Dieldrin (µg/L)	Dieldrin, Total (µg/L)	Disulfoton (µg/L)	D-Limonene (µg/L)	Endosulfan I, Total (µg/L)	Endrin (µg/L)	EPTC (µg/L)	Ethalfluralin (µg/L)	Ethoprop (µg/L)	Fipronil Degradate RPA105048 (µg/L)	Fipronil Sulfide (µg/L)	Fipronil Sulfone (µg/L)	Fipronil (µg/L)	Fluoranthene (µg/L)
05-14-01	<.005	<.005	--	<.02	--	--	--	0.011	<.009	<.005	--	--	--	--	--
06-19-01	<.005	<.005	--	<.02	--	--	--	<.002	<.009	<.005	--	--	--	--	--
08-21-01	<.005	<.005	<.006	<.02	--	<.02	<.01	<.002	<.009	<.005	--	--	--	--	--
10-17-01	<.5	<.005	--	<.02	<.5	--	--	<.002	<.009	<.005	--	--	--	--	<.5
04-08-02	<.005	<.005	--	<.02	<.5	--	--	<.002	<.009	<.005	--	--	--	--	<.5
08-27-02	<.005	<.005	<.006	<.02	<.5	<.02	<.01	<.002	<.009	<.005	--	--	--	--	<.5
10-18-02	<.005	<.005	--	<.02	--	--	--	<.002	<.009	<.005	<.009	<.005	<.005	<.007	--

Appendix 2. Concentrations of organic compounds in water samples from S-Line Canal collected from Cemetery Bridge, May 2001 to October 2002—Continued

Date	Fonofos (µg/L)	Heptachlor epoxide, Total (µg/L)	Heptachlor, Total (µg/L)	Hexahydro-hexamethyl-cyclopenta-benzopyran (µg/L)	Indole (µg/L)	Isoborneol (µg/L)	Isophorone (µg/L)	Isopropyl-benzene (Cumene) (µg/L)	Isoquinoline (µg/L)	Lindane (µg/L)	Lindane, Total (µg/L)	Linuron (µg/L)	Malathion (µg/L)	Menthol (µg/L)
05-14-01	<.003	--	--	--	--	--	--	--	--	<.004	--	<.035	<.027	--
06-19-01	<.003	--	--	--	--	--	--	--	--	<.004	--	<.035	<.027	--
08-21-01	<.003	<.009	<.01	--	--	--	--	--	--	<.004	<.006	<.035	<.027	--
10-17-01	<.003	--	--	M	<.5	<.5	E.3	<.5	<.5	<.004	--	<.035	<.027	<.5
04-08-02	<.003	--	--	<.5	<.5	<.5	<.5	M	<.5	<.004	--	<.035	<.027	<.5
08-27-02	<.003	<.009	<.01	<.5	<.5	<.5	1.8	<.5	<.5	<.004	<.006	<.035	<.027	<.5
10-18-02	<.003	--	--	--	--	--	--	--	--	<.004	--	<.035	<.027	--

Date	Metalaxyl (µg/L)	Methoxychlor, Total (µg/L)	Methyl-azinphos (µg/L)	Methyl-parathion (µg/L)	Methyl-salicylate (µg/L)	Metolachlor (µg/L)	Metribuzin, (Sencor) (µg/L)	Mirex Total (µg/L)	Molinate (µg/L)	N,N,-Diethyl-meta- Diethyl-toluamide (DEET) (µg/L)	Naphthalene (µg/L)	Napropamide (µg/L)	Diethoxy-nonyl-phenol (µg/L)	Diethoxy-octyl-phenol (µg/L)
05-14-01	--	--	<.050	<.006	--	<.013	<.006	--	<.002	--	--	<.007	--	--
06-19-01	--	--	<.050	<.006	--	<.013	<.006	--	<.002	--	--	<.007	--	--
08-21-01	--	<.020	<.050	<.006	--	<.013	<.006	<.006	<.002	--	--	<.007	--	--
10-17-01	<.5	--	<.050	<.006	<.5	<.5	<.006	--	<.002	M	<.5	<.007	<5	<1
04-08-02	<.5	--	<.050	<.006	<.5	<.013	<.006	--	<.002	E.1	<.5	<.007	<5	<1
08-27-02	<.5	<.020	<.050	<.006	<.5	<.013	<.006	<.006	<.002	E.1	<.5	<.007	<5	<1
10-18-02	--	--	<.050	<.006	--	<.013	<.006	--	<.002	--	--	<.007	--	--

Appendix 2. Concentrations of organic compounds in water samples from S-Line Canal collected from Cemetery Bridge, May 2001 to October 2002—Continued

Date	Mono-ethoxy-octyl-phenol (µg/L)	p,p'-DDE Total (µg/L)	p,p'-DDD, Total (µg/L)	p,p'-DDE, Total (µg/L)	p,p'-DDT, Total (µg/L)	Para-cresol (µg/L)	Para-nonyl-phenol (µg/L)	Para-thion (µg/L)	PCB Total (µg/L)	Peb-ulate (µg/L)	Pendi-methalin (µg/L)	Penta-chloro-phenol (µg/L)	Cis-perm-ethrin (µg/L)
05-14-01	--	<.003	--	--	--	--	--	<.007		<.002	<.010	--	<.006
06-19-01	--	<.003	--	--	--	--	--	<.007		<.002	<.010	--	<.006
08-21-01	--	<.003	<.007	<.006	<.009	--	--	<.007	<.1	<.002	<.010	--	<.006
10-17-01	<1	<.003	--	--	--	<1	<5	<.007		<.002	<.010	<2	<.006
04-08-02	<1	<.003	--	--	--	<1	<5	<.010		<.004	<.022	<2	<.006
08-27-02	<1	<.003	<.007	<.006	<.009	<1	<5	<.010	<.1	<.004	<.022	<2	<.006
10-18-02	--	<.003	--	--	--	--	--	<.010		<.004	<.022	--	<.006

Date	Phen-anthrene (µg/L)	Phenol (µg/L)	Phorate (µg/L)	Prometon (µg/L)	Pron-amide (µg/L)	Propachlor (µg/L)	Propanil (µg/L)	Propargite (µg/L)	Pyrene (µg/L)	Simazine (µg/L)	Stig-mastanol (µg/L)	Tebu-thiuron (µg/L)	Terbacil (µg/L)	Terbufos (µg/L)
05-14-01	--	--	<.011	M	<.004	<.010	<.011	<.02	--	<.011	--	<.02	<.034	<.02
06-19-01	--	--	<.011	<.01	<.004	<.010	<.011	<.02	--	E.002	--	<.02	<.034	<.02
08-21-01	--	--	<.011	<.01	<.004	<.010	<.011	<.02	--	<.011	--	<.02	<.034	<.02
10-17-01	<.5	E.3	<.011	<.5	<.004	<.010	<.011	<.02	<.5	<.011	<2	<.02	<.034	<.02
04-08-02	<.5	<.5	<.011	<.01	<.004	<.010	<.011	<.02	<.5	<.005	<2	<.02	<.034	<.02
08-27-02	<.5	E.4	<.011	<.01	<.004	<.010	<.011	<.02	<.5	<.005	<2	<.02	<.034	<.02
10-18-02	--	--	<.011	<.01	<.007	<.010	<.011	<.02	--	<.005	--	<.02	<.050	<.02

Appendix 2. Concentrations of organic compounds in water samples from S-Line Canal collected from Cemetery Bridge, May 2001 to October 2002—Continued

Date	Tetra-chloro-ethylene (µg/L)	Thio-bencarb (µg/L)	Toxa-phene, Total (µg/L)	Tri-(2-chloro-ethyl) phosphate (µg/L)	Tri-(dichlor-isopropyl)-phosphate (µg/L)	Tri-allate (µg/L)	Tributyl-phosphate (µg/L)	Triclosan (µg/L)	Triethyl-citrate (µg/L)	Trifluralin (µg/L)	Triphenyl-phosphate (µg/L)	Tris-(2-butoxy-ethyl)-phosphate (µg/L)	Dichlor-vos (µg/L)
05-14-01	--	<.005	--	--	--	<.002	--	--	--	<.009	--	--	--
06-19-01	--	<.005	--	--	--	<.002	--	--	--	<.009	--	--	--
08-21-01	--	<.005	<1	--	--	<.002	--	--	--	<.009	--	--	--
10-17-01	<.5	<.005	--	<.5	E.1	<.002	<.5	<1	<.5	<.009	M	E.2	<1.00
04-08-02	<.5	<.005	--	E.1	E.1	<.002	<.5	<1	<.5	<.009	<.5	E.2	<1.00
08-27-02	<.5	<.005	<1	M	M	<.002	<.5	<1	<.5	<.009	<.5	E.1	<1.00
10-18-02	--	<.005	--	--	--	<.002	--	--	--	<.009	--	--	--

Appendix 3. Reagents and analytical methods used for partial solution extractions

Water soluble and cation exchange capacity	
Reagents, analytical steps, and analytes	**Reference**
0.2 M NH_4Cl: Dissolve 107 g of NH_4Cl and make up to 10 L with deionized water.	Sumner and Miller (1996)
1. Weigh each rock sample and record. Take the entire amount for the analysis.	
2. Add the rock to a 1,000 mL beaker or erlenmeyer flask and add 300 mL of 0.2 M NH_4Cl.	
3. Shake gently on a gyaratory shaker for 1 hour. Slow the shaker speed so there is no attrition grinding.	
4. Decant the supernatant into a 2,000 mL volumetric flask.	
5. Add another 300 mL of 0.2 M NH_4Cl and shake for 1 hour as before.	
6. Decant the supernatant into the same 2,000 mL volumetric flask.	
7. Repeat steps 5 and 6 three more times for a total of five cycles.	
8. Make the final volume up to 2,000 mL. Filter an aliquot and analyze by ICP-ES (Na, K, Ca, Mg, Al, SiO_2 and As).	
9. Save the rock samples for anion exchange capacity.	

Anion exchange capacity	
Reagents, analytical steps, and analytes	**Reference**
0.2 M potassium nitrate 0.2 M KNO_3: Dissolve 202 g of KNO_3 and make up to 10 L with deionized water.	Sumner and Miller (1996)
1. Wash the rock with 300 mL of DI water. Shake gently on the gyratory shaker for 1 hour and discard the wash water by decanting off.	
2. Repeat step 1 two more times discarding the wash water each time.	
3. Weigh the rock to determine the quantity of entrained liquid. Record.	
4. Add 300 mL of 0.2 M KNO_3 and shake for 1 hour. Decant the supernatant into a 2,000 mL volumetric flask.	
5. Repeat Step 4 four more times for a total of 5 cycles.	
6. Make up the final volume to 2,000 mL and submit a filtered aliquot to chemistry for ammonia, total P, chloride and arsenic analysis.	
7. Save the rock samples for determination of the carbonate minerals.	

Appendix 3. Reagents and analytical methods used for partial solution extractions—Continued

Carbonate minerals	
Reagents, analytical steps, and analytes	**Reference**
1 M sodium acetate, adjust to pH = 5.0 with acetic acid 1M sodium acetate: dissolved 410 g of $NaC_2H_3O_2$ in 4 L of DI water. Adjust to pH 5.0 with glacial acetic acid. Makeup to a final volume of 5.0 L.	Tessier and others (1979)
1. To each rock sample add 300 mL of pH 5 solution and shake slowly on a gyratory shaker for 6 hours. Check the pH after 3.0 hours. If it is >5.5 decant the solution. Pour the decant into a 2 L volumetric flask and analyze a small filtered aliquot for calcium.	
2. Add a fresh 300 mL aliquot to the rock and agitate overnight 16 hours. Analyze a small filtered aliquot for calcium and decant the remaining solution into a 2 L volumetric flask.	
3. Repeat Step 2 for an additional 6-hours and 16-hour period, if required, until the quantity of calcium decreases indicating minimal carbonate dissolution. Save the rock samples for determination of the iron oxide fraction.	
4. Makeup the combined extracts to a final volume of 1,000 or 2,000 mL depending on the number of extracts.	
5. Analyze a filtered aliquot for Ca, Mg, total P, SiO_2, Al and As.	
6. Save the rock samples for determination of iron and manganese oxide fraction.	

Iron and manganese oxides	
Reagents, analytical steps, and analytes	**Reference**
Hydroxylamine hydrochloride in 25 percent (v/v) acetic acid 0.04 M hydroxylamine hydrochloride: dissolve 11.12 g of $NH_2OH.HCl$ and add 25 percent acetic acid (v/v) until the pH is ~2.0. Makeup to a final volume of 4.00 L.	Tessier and others (1979)
1. To each rock sample add 300 mL of solution and shake slowly on a gyratory shaker for 6 hours. Decant the solution into a 2 L volumetric flask and analyze a small aliquot for iron.	
2. Add another 300 mL aliquot and again agitate for 16 hours. Analyze and save a small aliquot for iron analysis and decant the remaining solution into a 2 L volumetric flask.	
3. Repeat Step 2 for an additional 6-hour and 16-hour period, if required, until the quantity of iron decreases indicating minimal oxide dissolution.	
4. Analyze the first extract solution for SO_4, Fe, Mn, total P, SiO_2, Al and As.	

Welch—Characterization of Surface-Water Quality in the S-Line Canal, Basalt Aquifer near Fallon, Nevada — Scientific Investigations Report 2005–5102